AD-A111 536 UNIVERSITY OF SOUTHERN CALIFORNIA LOS ANGELES CENTER--ETC F/G 20/6
LOW LOSS OPTICAL WAVEGUIDES IN GLASS FABRICATED BY ELECTRIC FIE--ETC(U)
NOV 81 E GARMIRE, K E WILSON F49620-80-C-0099

UNCLASSIFIED AFOSR-TR-81-0898 NL

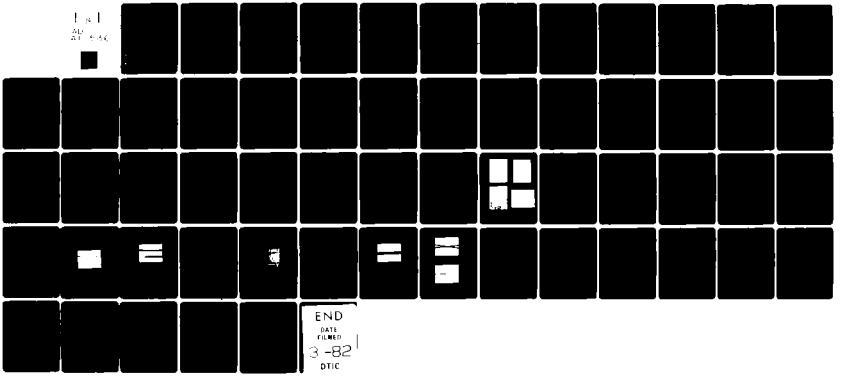

END
DATE FILMED
3-82
DTIC

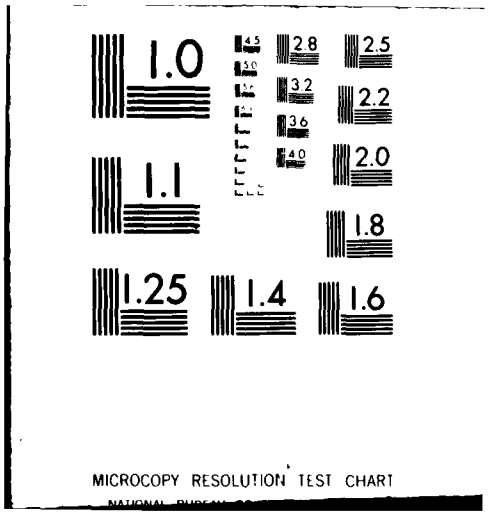
1.0
1.1
1.25
1.4
1.6
1.8
2.0
2.2
2.5
2.8
3.2
3.6
4.0
4.5
5.0
MICROCOPY RESOLUTION TEST CHART

REPORT DOCUMENTATION PAGE

READ INSTRUCTIONS BEFORE COMPLETING FORM

1. REPORT NUMBER: AFOSR-TR- 81-0898	2. GOVT ACCESSION NO: AD-A111 536
3. RECIPIENT'S CATALOG NUMBER	
4. TITLE (and Subtitle): LOW LOSS OPTICAL WAVEGUIDES IN GLASS FABRICATED BY ELECTRIC FIELD ASSISTED DIFFUSION FROM SILVER FILMS	5. TYPE OF REPORT & PERIOD COVERED: Final Aug'80 - Sept'81
	6. PERFORMING ORG. REPORT NUMBER
7. AUTHOR(s): E. Garmire and K.E. Wilson	8. CONTRACT OR GRANT NUMBER(s): F49620-80-C-0099
9. PERFORMING ORGANIZATION NAME AND ADDRESS: Center for Laser Studies, University of Southern California, Los Angeles, CA 90007	10. PROGRAM ELEMENT, PROJECT, TASK AREA & WORK UNIT NUMBERS: 61102F 2305/B2
11. CONTROLLING OFFICE NAME AND ADDRESS: AFOSR/NE, Building 410, Bolling AFB, DC 20332	12. REPORT DATE: November 25, 1981
	13. NUMBER OF PAGES: 55
14. MONITORING AGENCY NAME & ADDRESS (if different from Controlling Office)	15. SECURITY CLASS. (of this report): Unclassified
	15a. DECLASSIFICATION/DOWNGRADING SCHEDULE

16. DISTRIBUTION STATEMENT (of this Report)

Approved for Public Release; Distribuition Unlimited

17. DISTRIBUTION STATEMENT (of the abstract entered in Block 20, if different from Report)

18. SUPPLEMENTARY NOTES

19. KEY WORDS (Continue on reverse side if necessary and identify by block number)

Integrated Optics
Waveguides
Glass

20. ABSTRACT (Continue on reverse side if necessary and identify by block number)

This report describes continuing research in fabricating low loss glass waveguides for an integrated optics ring interferometer to be used for inertial rotation sensing. During this year progress was made in identifying the losses which occur during diffusion of a waveguide into glass. We developed special optical glass in which we were able to diffuse waveguides with losses which are four times smaller than observed in preliminary

DD FORM 1 JAN 73 1473

20. Cont'd

experiments in microscope slides. From its mode-dependence, we were able to determine that the residual loss is due to roughness of the surface introduced by the silver during the diffusion.

We introduced the technique of laser writing of masks for integrated optics and succeeded in writing a ring channel mask 10 cm in diameter and 10 μm wide. The combination of this mask and a straight-line mask provide the capability for producing a ring interferometer of dimensions required for inertial rotation sensing. We have also demonstrated that photoacoustic spectroscopy may be a very useful tool for determining the silver depth profiles in a nondestructive fashion.

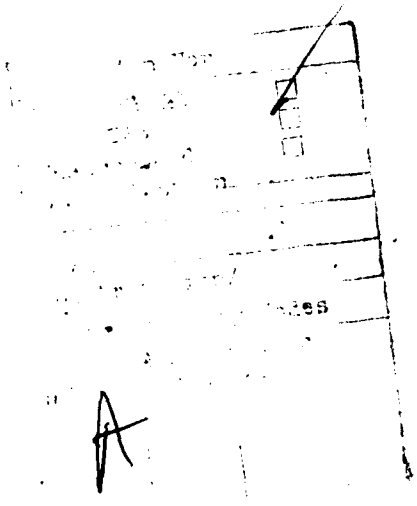

TABLE OF CONTENTS

	Page
Abstract	i
Table of Contents	ii
1. INTRODUCTION	1
1.1 Milestones Achieved This Year	1
1.1.1 Fabrication of Waveguides and Reduction of Loss in Optical Glasses Without Fining Agents	1
1.1.2 Fabrication of Waveguides with Loss Below Measurable Limits in S3 Glass Without Titanium	1
1.1.3 Fabrication of Low-loss Waveguides in S2 Glass Using Field-assisted Diffusion	1
1.1.4 Reduction of Loss for Field-assisted Waveguides	2
1.1.5 Buried Waveguides in S3 Glass Using Two-Step Field-Assisted Diffusion	2
1.1.6 Fabrication of Straight and Channel Waveguides	2
1.1.7 Laser Writing of a Directional Coupler and 4 μm stripes	2
1.1.8 Fabrication of Narrow Channel Waveguides	3
1.1.9 Fabrication of Waveguide Directional Couplers	4
1.1.10 Fabrication of Ring Interferometer	4
1.1.11 Photoacoustic Detection of Waveguide Profile	4
1.2 Information Dissemination	6
1.3 Personnel Involved in the Program	8
2. TECHNICAL DEVELOPMENT	9
2.1 Low-Loss Optical Waveguide Fo[illegible]n by Field-Assisted Solid-State Diffusion of [illegible]etals in Glass	10
2.2 Additional Data Pertinent to Milestones	17
2.2.1 Low-Loss Waveguides in S3 Glass Without Titanium	17
2.2.2 Field-Assisted Diffusion in S2 and S8000	21
2.2.3 Laser Writing of Narrow Lines and Parallel Channels	30
2.2.4 Laser Writing of Masks	33

TABLE OF CONTENTS (Cont'd)

Page

2.2.5 Groove/ridge Formation in Field-Assisted Diffusion 47

3. ADDITIONAL RESULTS 49

3.1 Photoacoustic Measurement of Refractive Index Profile in Glass Waveguides 49

3.1.1 Introduction 49

3.1.2 Results

3.2 Attempts to Diffuse Waveguides into Quartz 55

1. INTRODUCTION

1.1 MILESTONES ACHIEVED THIS YEAR

The research in the past year was characterized by the milestones shown in Fig.1.1. These milestones were divided into two main areas of research: a continuation of the reduction of loss in the waveguides, and a development of the ring interferometer through laser writing. The milestones shown in Fig.1.1 are briefly described below.

1.1.1 Fabrication of waveguides and reduction of loss in optical glasses without fining agents.

The first year of the program we discovered that using commercially available optical glasses as substrates resulted in waveguides which were more lossy than those fabricated in microscope slides. In order to achieve the first milestone, we obtained specially prepared Schott optical glasses without arsenic, their usual fining agents. We fabricated waveguides in these glasses and observed the mode-dependence of the loss in order to determine its cause. The results are described in section 2.1. In summary, S8000 glass showed scatter losses the order of 0.2dB/cm, while the S3 glass showed no scatter loss, but considerable absorption loss, due to the presence of titanium. We therefore ordered a new batch of S3 glass without titanium.

1.1.2 Fabrication of waveguides with loss below measurable limits in S3 glass without titanium.

The second milestone was achieved when we demonstrated that the loss in thermally diffused silver waveguides in S3 glass, fabricated without arsenic or titanium, was less than could be measured with the three prism coupling method (0.1dB/cm). These results are described in section 2.2.1, and were presented at the Optical Society annual meeting in Florida.

1.1.3 Fabrication of low-loss waveguides in S3 glass using field-assisted diffusion.

The ring interferometer requires waveguides with a sufficiently high refractive index compared to that of the substrate so that radiation loss in the ring guide will be negligible. Higher refractive index changes are achieved by increasing the effectiveness of thermal diffusion with the assistance of an electric field. Two-mode waveguides have now been fabricated with

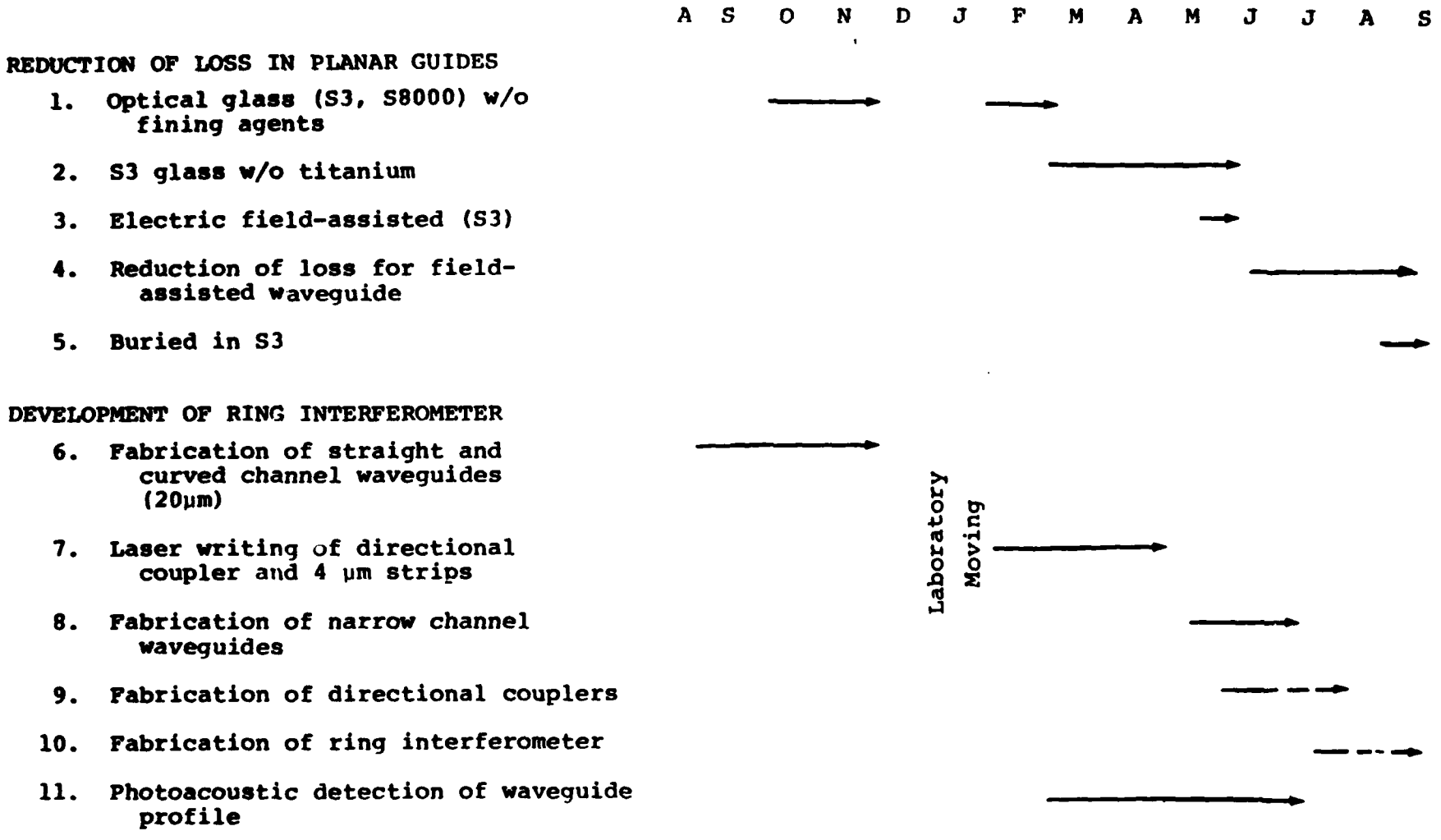

Figure 1.1 Milestones in the program

sufficiently high refractive index to be useful for the ring interferometer.

1.1.4. Reduction of loss for field-assisted waveguides

The field assisted waveguides fabricated in May and June were found to have considerably more loss than the thermally diffused waveguides. Experimentation determined that this was due to the gold electrodes which were used during the diffusion. We changed our technique, therefore, and found that with a sufficiently thick silver layer, no additional contact was required. This new technique reduced the losses to a factor of six.

1.1.5 Buried waveguides in S3 glass using two-step field-assisted diffusion.

In the first year of the program we demonstrated that reintroducing the waveguide to a second field-assisted diffusion in the absence of residual silver oxide caused the waveguide to be buried below the surface and reduce the loss substantially. We have recently introduced an annealing step and demonstrated that the losses may be lower than without it. Some preliminary evidence indicates that under some conditions these waveguides may be buried, although conclusive results were not obtained before the contract ran out.

1.1.6 Fabrication of straight and channel waveguides

Simultaneous to the development of low-loss planar waveguides has been the development of laser writing techniques for the straight and curved channel waveguides required by the ring interferometer. The first milestone in this program was to fabricate both straight and curved channel waveguides. This was achieved by November, for channels which were relatively wide (10-20 μm), dimensions for which optical alignment and photoresist processing are not critical. Results are outlined in section 2.1.

1.1.7 Laser writing of a directional coupler and 4 μm stripes

Wide channels are multimode and also subject to high radiation losses in the ring. Fabrication of sufficiently narrow waveguides to be applicable to the single mode technology of the ring interferometer required considerable refinements to the technology of

fabrication. For this reason, a separate milestone was the ability to fabricate silver strips 4 μm wide and directional coupler circuits with 6 μm spacing. This milestone was achieved by careful control of time and temperature during etch, and by introducing an optical interferometer on the laser writing apparatus so that the separation between the curved and straight channels in the directional coupler can be measured in units of wavelength. The results are shown in section 2.2.3.

Because successful laser writing required careful control of the process, we decided the more efficient results would be obtained by writing a master mask and replicating it on the substrates using standard photoresist techniques. We were successful in writing good quality masks using the laser, and our results are being published in the IEEE Transactions.

1.1.8 Fabrication of narrow channel waveguides

This is a separate milestone because after the appropriate optical circuit has been defined in silver, the electric field-assisted diffusion of a single mode guide must be completed, and techniques developed to demonstrate the optical waveguide properties. We fabricated multimode channel waveguides 20 μm wide, and observed waveguiding in them. We were not able to fabricate thinner waveguides with our original technique, because of problems delineating the narrow silver stripe with etching. We therefore decided to use a metallic mask as a barrier to the silver diffusion. Experiments with delineating the optical circuit in titanium were successful.

Problems with the formation of grooves and ridges during diffusion also hindered our observation of narrow channel waveguides. It was decided to use end-fire coupling to observe narrow channel waveguides, and this required polishing the end faces of the glass substrates. We are currently developing the capability to polish endfaces of integrated optical circuits.

1.1.9 Fabrication of waveguide directional couplers.

In the course of experimentation we found that it was more difficult to fabricate directional couplers directly by laser writing than had first been anticipated. This is because of severe alignment requirements needed to avoid intersections between the straight line and the circle. After several attempts to perfect the laser writing stage to include autoalignment for directional couplers, we decided to utilize separate ring and straight-line masks and to print both on the substrate, aligning them carefully with the mask aligner. This requires iron oxide semi-transparent masks which we had not been using. However, we had our best straight and ring masks replicated by a commercial vendor onto iron oxide masks. Time ran out in the program, however, before we were able to test them on samples in the mask aligner.

1.1.10. Fabrication of ring interferometer

We used laser writing to fabricate a ring mask 10 μm wide and 10 cm in diameter. This ring mask will be suitable for the fabrication of ring waveguides. We made initial efforts to fabricate curved channel waveguides using thermal diffusion, but were not successful in our efforts to observe waveguiding. At this stage we are not certain whether the lack of success was due to insufficient refractive index change, or to problems with coupling into the waveguide. Systemmatic studies were underway at the end of the contract to determine which of these two possibilities was the reason.

1.1.11 Photoacoustic detection of waveguide profile

A separate task which we initiated to a limited extent during part of the year was the use of photoacoustic spectroscopy to detect and measure silver diffusion profiles in the glass waveguides. Preliminary experiments were successful and suggest that the development of this technique may have several useful applications. This initial work resulted in a paper which was presented at the Second International Topical Meeting on Photoacoustic Spectroscopy in June.

1.2 INFORMATION DISSEMINATION

Publications:

1. "Reduction and control of optical waveguide losses in glass", T. Findakly and E. Garmire, Appl. Phys. Lett. 37, 855 (1980)

2. "Low-Loss Optical Waveguide Formation by Field-Assisted Solid-State Diffusion of Metals in Glass" K. Wilson, K. Cheng, E. Garmire and T. Findakly, Proc. SPIE, vol. 269 (1981)

3. "Laser Writing of Masks for Integrated Optical Circuits" K. Wilson, C. Mueller, E. Garmire, IEEE Trans. on Components, Hybrids and Manufacturing Technology, special issue-section dealing with Fabrication and Evaluation of Integrated Optical Circuits. accepted for publication

Formal Presentations:

1. "Low-Loss Optical Waveguide Formation by Field-Assisted Solid-State Diffusion of Metals in Glass" SPIE, Los Angeles, February, 1981 (Presented by K. Wilson)

2. "Photoacoustic Measurement of Refractive Index Profile in Glass Waveguides" K. Cheng, R. Swimm, P. Yeung, Second International Topical Meeting on Photoacoustic Spectroscopy, Berkeley, June, 1981

3. "Comparison of Glass Waveguide Loss Using Different Substrates" K. E. Wilson, E. Garmire, R.M.Silva, W.K. Stowell. Presented at the Optical Society of America Annual Meeting, Florida, October, 1981

Informal Presentations:

1. Air Force Avionics Laboratory: Kent Stowell
   Robert Silva (properties of glass, surface smoothness, effects of fining agents, gyro applications)

2. Northrop Corporation: Tony Lawrence, Dr. Havistock, (comparison of passive ring resonators)

3. Rochester University: Duncan Moore (Gradient Index Optics, and its relation to diffused waveguides)

4. Hughes Research Laboratory: H.W. Yen, G. Tangonan (multimode and single mode glass waveguides, comparison of ion exchange from the melt and from silver films)

5. TRW: Talal Findakly (low loss waveguides, effect of fining agents, comparison of diffusion from the melt and from thin films)

6. Schott Glass: Dr. Mader (effect of fining agents in glass, preparation of special glass melts with specified ingredients)

7. Lear Siegler: H. Gubbins and R. Fredericks (gyro applications)

8. Stanford University: Prof. Shaw (gyro applications)

1.3 PERSONNEL INVOLVED IN THE PROGRAM

Principal Investigator:
E. Garmire (25%)

Research Scientists:
K. Cheng (50%)
K. Wilson (50%)

Students:

C. Mueller

Secretaries and Administrative
M. Ikegami
H. Fermanian

2. TECHNICAL DEVELOPMENT

2.1 LOW-LOSS OPTICAL WAVEGUIDE FORMATION BY FIELD-ASSISTED SOLID-STATE DIFFUSION OF METALS IN GLASS

Very low loss waveguides were fabricated in glass by thermal ion exchange from a thin film of silver vacuum deposited on the substrate. Planar and channel guides were made both with and without an applied electric field. By measuring the mode, wavelength and thickness dependence of the loss, the primary causes of loss in the guide were identified for several different glass substrates.

Very low loss ($\approx 10^{-1}$ dB/cm) optical waveguides have been fabricated by thermal migration of silver ions in glass. The initial studies using this technique were published in Reference 1. A thin film of silver ($\approx$2000 Å) was vacuum deposited on a glass substrate and ion exchange ($Ag^{+} \rightarrow Na^{+}$) was accomplished by heating the sample to temperatures between 300°C and 500°C. Diffusion times ranged from 10 minutes to three hours, resulting in guides with thicknesses from 10 μm to 100 μm. Mode angle measurements indicated that the index change Δn was approximately 10^{-3}. Larger index changes ($\Delta n \sim 10^{-2}$) were achieved by applying an electric field during diffusion. This paper reports results for several different glass substrates.

Two sources of loss in optical waveguides are those arising from surface roughness and those due to the concentration of diffused silver. Both these sources of loss have the same thickness-dependence. That this is so can be seen from the fact that thicker waveguides result in smaller evanescent fields at the surface and smaller silver concentration and thus less silver-dependent loss. Typical experimental results are shown in Fig. 2.1.A. The reduction of loss with increasing waveguide thickness is apparent. This fact is important to consider when low loss waveguides are reported. Numbers for waveguide loss should not be compared without specifying the waveguide thickness.

To identify the predominant loss mechanism in our guides, we measured the mode dependence of the losses. When the major source of loss is silver-concentration dependent, then the higher order modes which have deeper penetration will encounter less silver and therefore will be less lossy than the lower order modes. However, if the primary loss mechanism is surface roughness, the higher

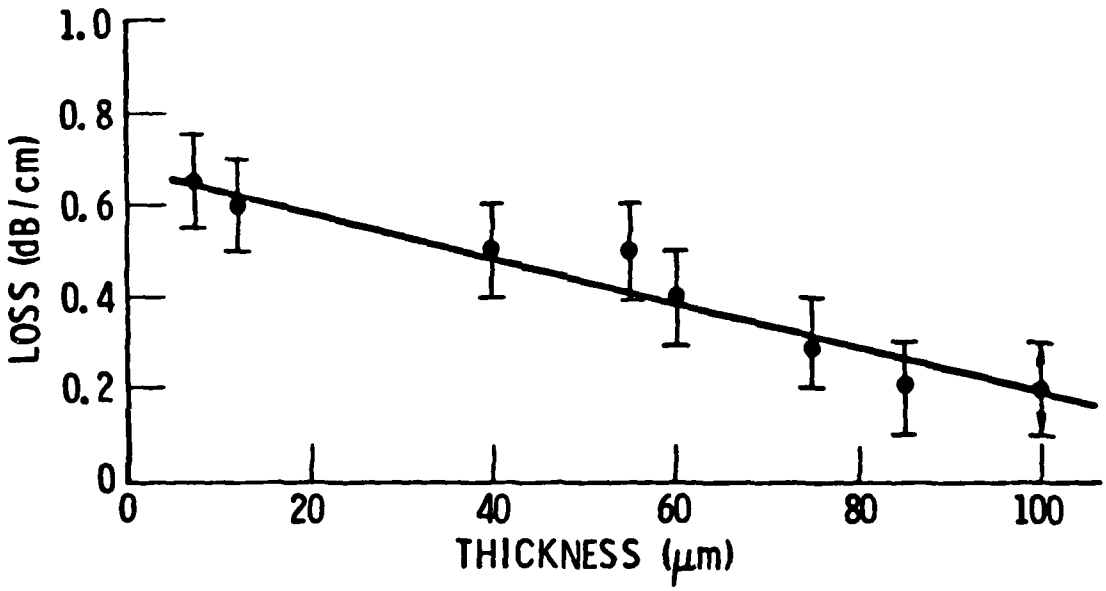

Fig. 2.1.A Thickness-dependent losses in waveguides formed by thermal ion exchange in glass.

order modes are the more lossy. Loss measurements were made using the scanning fiber probe method. The guided mode was excited by prism coupling and the light scattered in that mode was detected by a photomultiplier placed at the end of a 2mm diameter fiber-bundle. The probe was scanned along the length of the guide using a motor-driven translational stage. The detector output was recorded and the loss was calculated from the decrease in scattered intensity along the guide. To ensure no mode switching, the output of the excited mode was monitored during the experiment.

Mode dependent losses in guides fabricated using soda-lime silicate microscope slides were first made at three wavelengths as shown in Fig. 2.1.B. In the blue the losses are strongly silver-dependent. Fining agents frequently found in these glasses can reduce the silver ions to silver atoms. These atoms form colloidal centers of metallic silver which can both absorb and scatter light. Notice that at 1.15 μm the slope of the mode-dependent losses is reverse that in the blue. This indicates that the silver dependence of the loss at 1.15 μm is negligible and the residual 0.5 dB/cm loss is predominantly due to surface roughness. The losses at 0.633 μm, although significantly less than those at 0.476 μm, still are due primarily to silver concentration.

Fig. 2.1.C shows the mode dependence of the losses for waveguides fabricated in four glasses. Silver diffusion in the V1, S-3 and S-8000 samples was done at 400°C for 1 hour and at 500°C for 2 hours in sample K1. From mode dispersion measurements and WKB analysis we determined the effective thickness of the guides to be 60 μm, 67 μm, 28 μm, and 85 μm for V1, S-3, S-8000 and K1 respectively. The slope of the graph for the commercially available soda-lime silicate glasses (V1, K1) indicates that the losses are silver-concentration dependent. The more lossy K1 slide exhibited a yellow coloration after diffusion. SEM (Edax) analysis indicated there were traces of iron in Sample K1 which were not found in V1. The coloration of sample K1 is most likely caused by a chemical reaction between the silver ions and such fining agents as iron[2] found in this glass. The low-loss Schott optical glass S-3 has small amounts of titanium

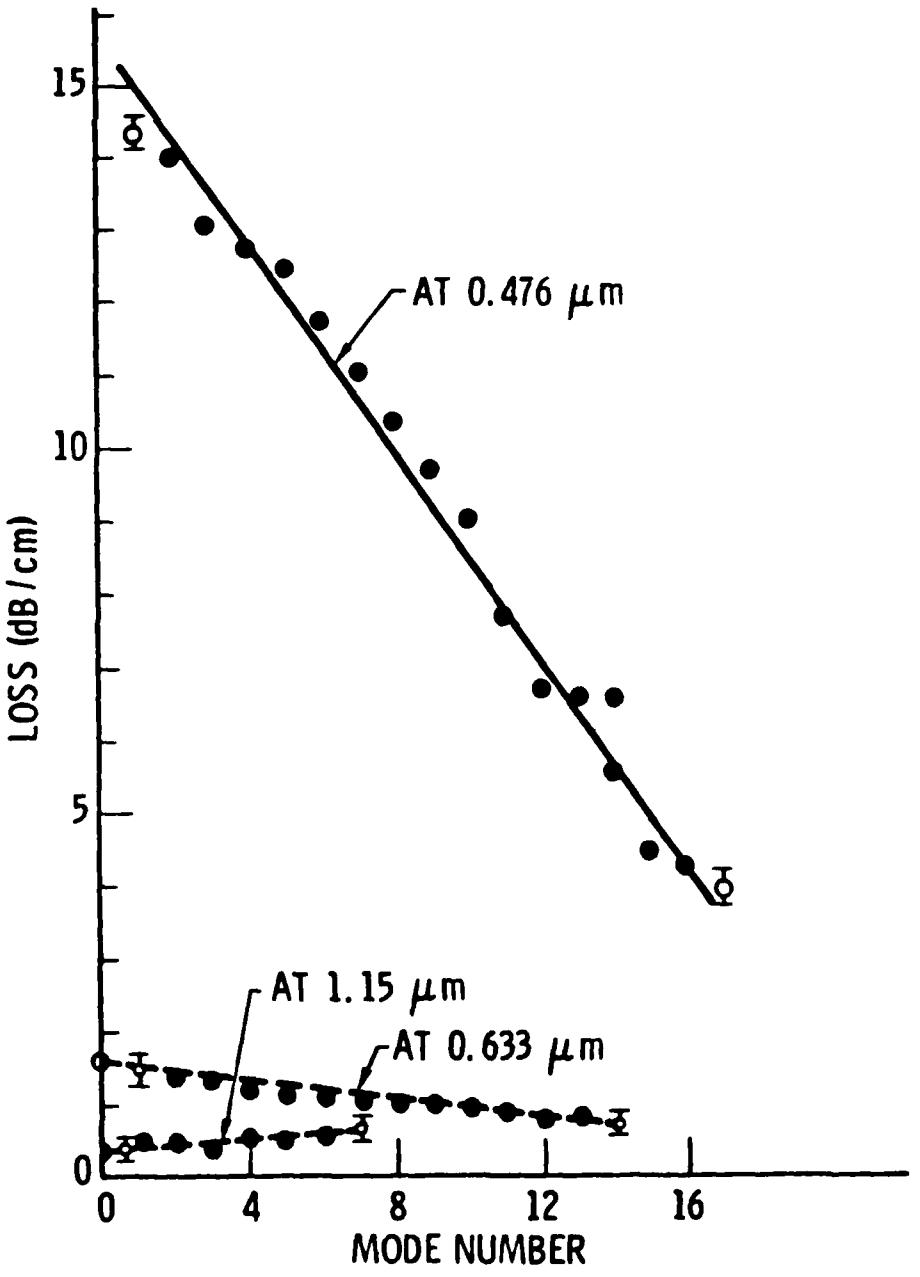

Fig. 2.1.B Mode-dependent losses at 0.476 μm, 0.633 μm, and 1.15 μm wavelengths in electro-diffused waveguides.

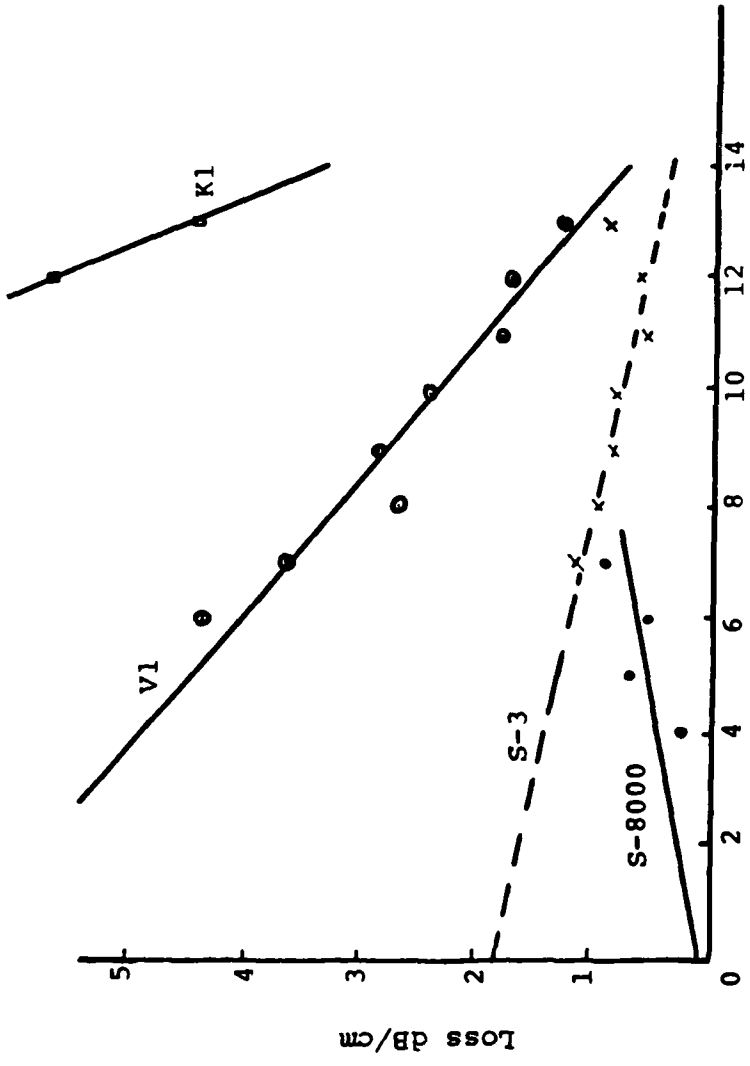

Fig. 2.1.C Mode-dependent losses for microscope slides V1 and K1 and optical glasses, S-8000 and S-3.

while there is none in the aluminum phosphate. Loss measurements done on these two glasses indicate, Fig. 2.1.C, that the losses are due to scattering in the S-8000, and to silver concentration in the S-3.

Waveguide channels were fabricated by laser beam writing with photo-resist techniques. The silvered surface of the substrate was spin coated with a thick layer of photo-resist. The photo-resist was exposed by focusing the 0.46 μm line of an Ar^+ laser on to the sample placed on a motor-driven translational and rotational stage. To ensure smooth edges during laser writing, the beam was spatially filtered and collimated before focusing. The width of the channel was controlled by varying the laser power and writing speed. After developing, the silver beneath the unexposed photoresist was etched using a solution of Cr_2O_3 in dilute H_2SO_4. Table 1 gives results of three channel guides fabricated by laser writing for diffusion temperatures ranging from 250°C - 500°C. Electric field assisted diffusion (samples DC6 and DCE) was accomplished by depositing gold electrodes on both sides of the substrate after the silver channel

Table 1

SAMPLE	WIDTH OF SILVER CHANNEL μM	TEMP. OF DIFFUSION °C	DIFFUSION TIME	E VOLTS/MM	RADIUS OF CURVATURE	# MODES
1 (KSDT1)	~30	500	2 HRS	0	∞	4 - 5
2 (DC6)	~10 - 20	300	13 MIN	60	∞	4
3 (KSDCE)	~40	250	1 HR	100	5°	6

was written. Results of WKB[1] analysis give $\Delta n \simeq 1.6 \times 10^{-2}$ and $z \simeq 8$ μm. In some samples it was found that, after electrodiffusion and etching, the channels were visible under a microscope. This indicated that there was a height change at the location of the channel. Profilometer measurements showed that, converse to $LiNbO_3$ channel guides, there was a depression at the original position of the silver, Fig. 2.1.D. The depth and width of this groove (Table 2) showed a strong dependence on the diffusion time. Experiments are currently being performed to determine the mechanism of groove formation.

Table 2

SAMPLE	WIDTH OF SILVER CHANNEL μM	TEMP. OF DIFFUSION (°C)	DIFFUSION TIME	E VOLTS/MM	GROOVE WIDTH μM	GROOVE DEPTH Å
1 (DC1)	~10 - 20	400	3.5 HRS	90	~60	3000 - 4000
2 (DC2)	~10 - 20	400	36 MIN	100	~38	~2000
3 (DC3)	~10 - 20	300	18.5 MIN	100	~5	~500

References

1. T. Findakly, and E. Garmire, "Reduction and Control of Optical Waveguide Losses in Glass, " Appl. Phys. Lett. 37, 855 (1980).
2. J. E. Midwinter, Optical Fibers for Transmission 1979.

This section is a preprint of a paper to be published in SPIE, vol. 269, 1981. The authors are K. Wilson, K. Cheng, E. Garmire and T. Findakly.

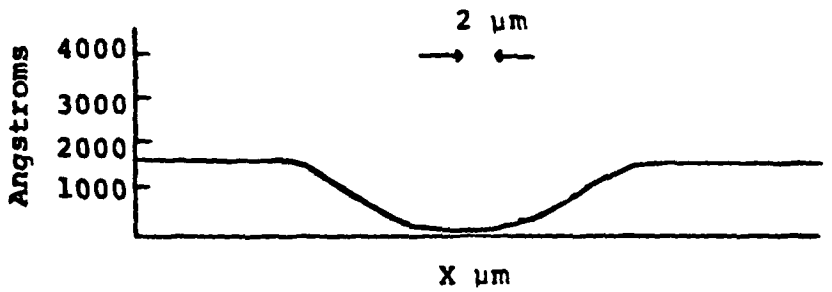

Fig. 2.1.D Typical profilometer trace of groove formed when electro-diffusion is done at elevated temperatures. X is position measured along glass surface.

2.2 ADDITIONAL DATA PERTINENT TO MILESTONES

2.2.1 Low-Loss Waveguides in S3 Glass Without Titanium

Thermally diffused waveguides were made in S3 glass, specially prepared without arsenic or titanium. Diffusion was from a 2000Å silver film at 400°C for 60 min. The result was a 13 mode guide with a loss reduced by a factor of 5 from the S3 glass fabricated with titanium.

The refractive index profile, determined by the WKB method from the prism coupling angles, is shown in Fig. 2.2.1.A. The large error bars are typical of multi-mode waveguides.

The loss was measured using a three-prism method. This technique was developed because the scanning fiber probe was not sensitive enough to detect any measurable loss. The three-prism method utilizes one input prism and two output prisms and has an estimated accuracy of 0.1 dB/cm. Figure 2.2.1.B shows the prism arrangement. The light coupled into the guide is coupled out at prism 1 and the remaining light is coupled out at prism 2. By adjusting the pressure on prism 1, the signal at prism 2 can be adjusted until it is within the linear range of our detector. With the input prism and output prism 2 fixed, prism 1 is translated along the length of the guide and the output of this prism is measured as a function of its position from the input prism. The scheme is in essence a two-prism technique with the third prism serving as a monitor of the coupling efficiency at prism 1.

Shown in Figure 2.2.1.C is the mode dependence of the loss for the last five modes of sample B3T1 (400°C, 60 min.) as measured by the three prism coupling scheme. The error bars indicated in the figure represent the standard deviation of the loss measured with the probe beam incident at different positions on the input prism, and do not necessarily include all systematic errors. It is not possible at this early stage in the measurements to tell whether the apparent mode dependence is real, or a result of too few data points. For mode number smaller than 9, the coupling efficiency was too small for the signal to be above the noise limit of the detector, and meaningful loss measurements could not be made for these modes.

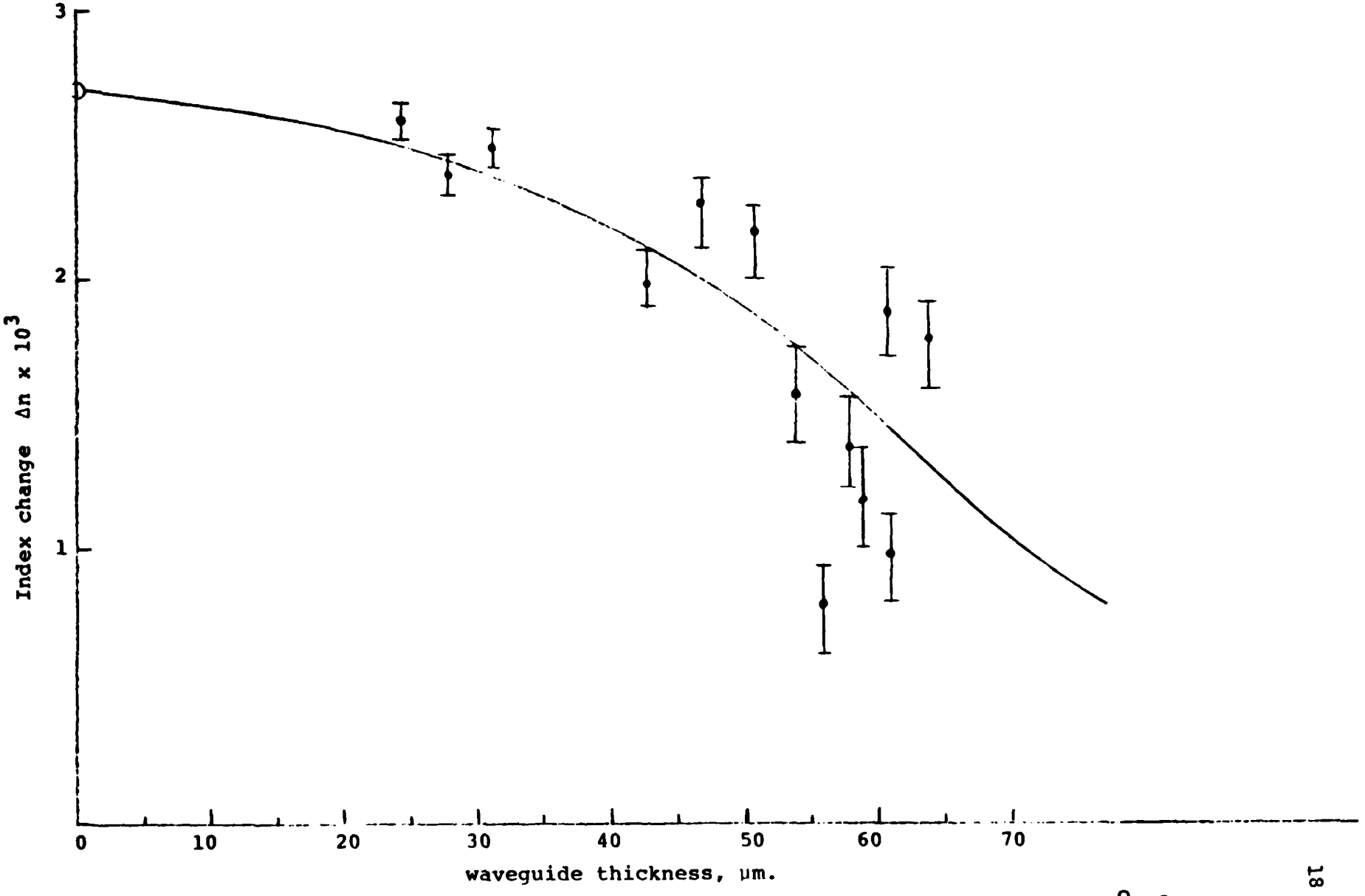

Fig. 2.2.1.A Index profile of waveguide fabricated by thermal diffusion at 400°C for 1 hour in S-3 glass.

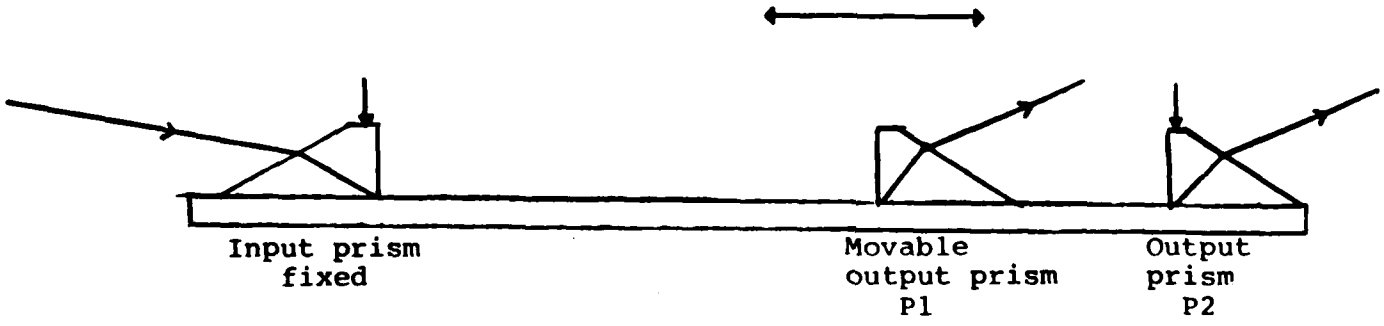

Fig. 2.2.1.B Losses are measured using the three prism coupling scheme shown. With the input coupler and P2 fixed, the intensity coupled out at P1 is recorded as a function of distance from the input prism.

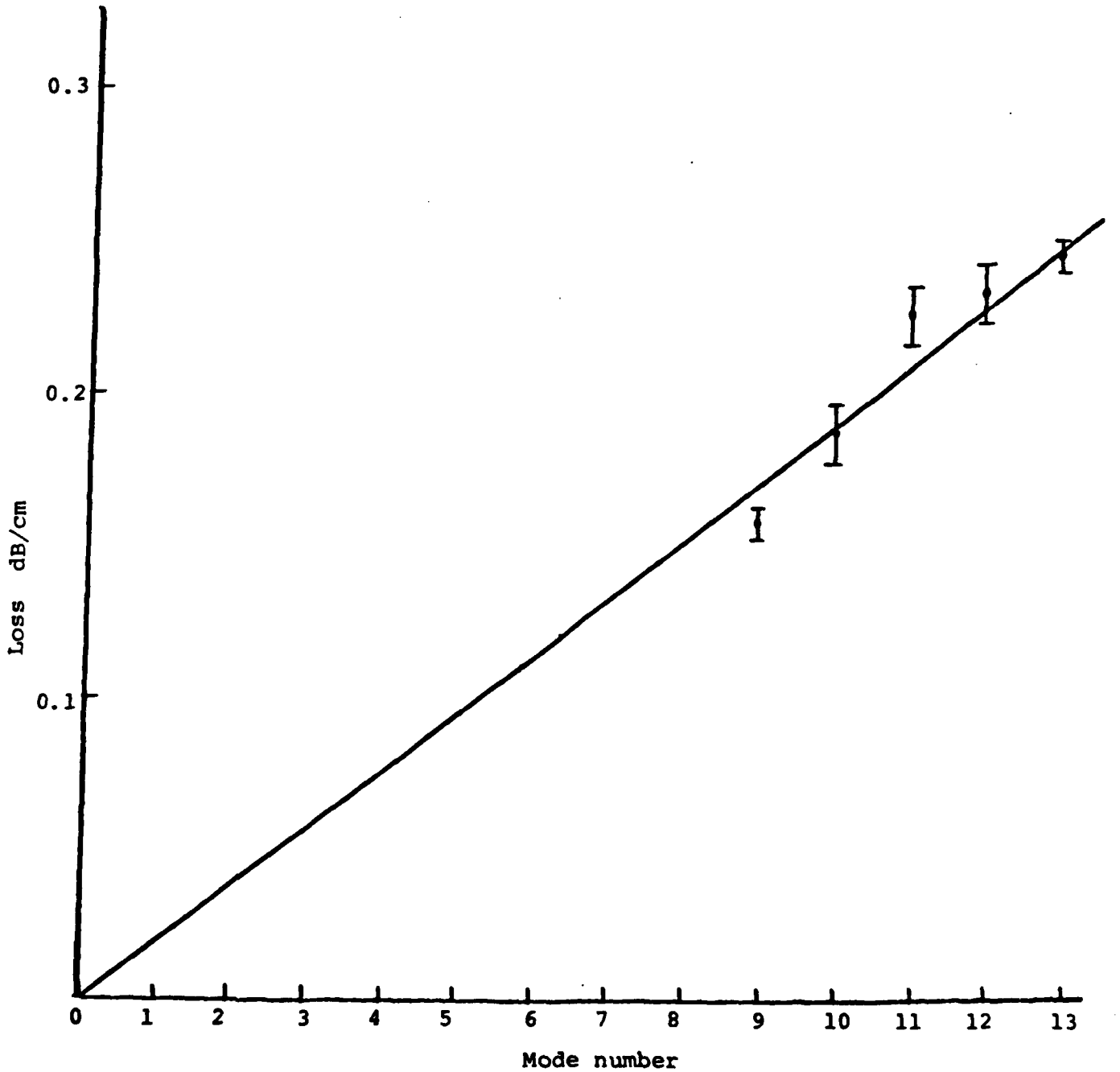

Fig. 2.2.1.C Mode dependent losses in S3 glass without arsenic or titanium.

2.2.2 Field-Assisted Diffusion in S3 and S8000

Field assisted diffusion was done using several samples of Schott S-8000 and S-3 glasses. The propagation constants for the various modes were determined from mode angle measurements and the index profile was fitted using W.K.B. analysis. Figure 2.2.2A shows the results for a 9 mode guide fabricated in S-3 glass at 400°C with a field of 40 V/mm applied for 15 min. The error bars represent the standard deviation in Δn and z determined from mode angle measurements at 5 different coupling positions along the face of the input prism. The index profiles for waveguides fabricated in S-8000 at lower temperatures and shorter diffusion times (Fig. 2.2.2B) indicate that Ag ion migration is much more rapid in this glass than in S3.

Because of its lower scattering, slower ion migration rate and low loss (with the removal of titanium) we concentrated on determining the parameters for single mode waveguide fabrication in S3. Table 2.2.2 gives the dependence of Δn, the number of modes, and waveguide thickness on the applied field and diffusion temperature with the field applied for 15 min.

TABLE 2.2.2

Temp °C	Field volts/mm	Time min.	Number of Modes	Depth z, μm	Δn WKB
400°C	40	15	9	19	0.02
350°C	40	15	4	5	0.03
350°C	20	15	3	5.5	0.016
350°C	5	15	2	4.7	0.007
350°C	2	15	1	--	(.004)

It can be seen that the guide depth and number of modes are relatively insensitive to the field strength and strongly sensitive to temperature. The temperature dependence of these

is shown in Fig. 2.2.2.C.

The last row in Table 2.2.2 gives the parameters used to obtain a single mode guide. Because WKB requires at least two modes to estimate guide parameters, Δn cannot be determined for a single mode. However, by extrapolating the curve for Δn as a function of

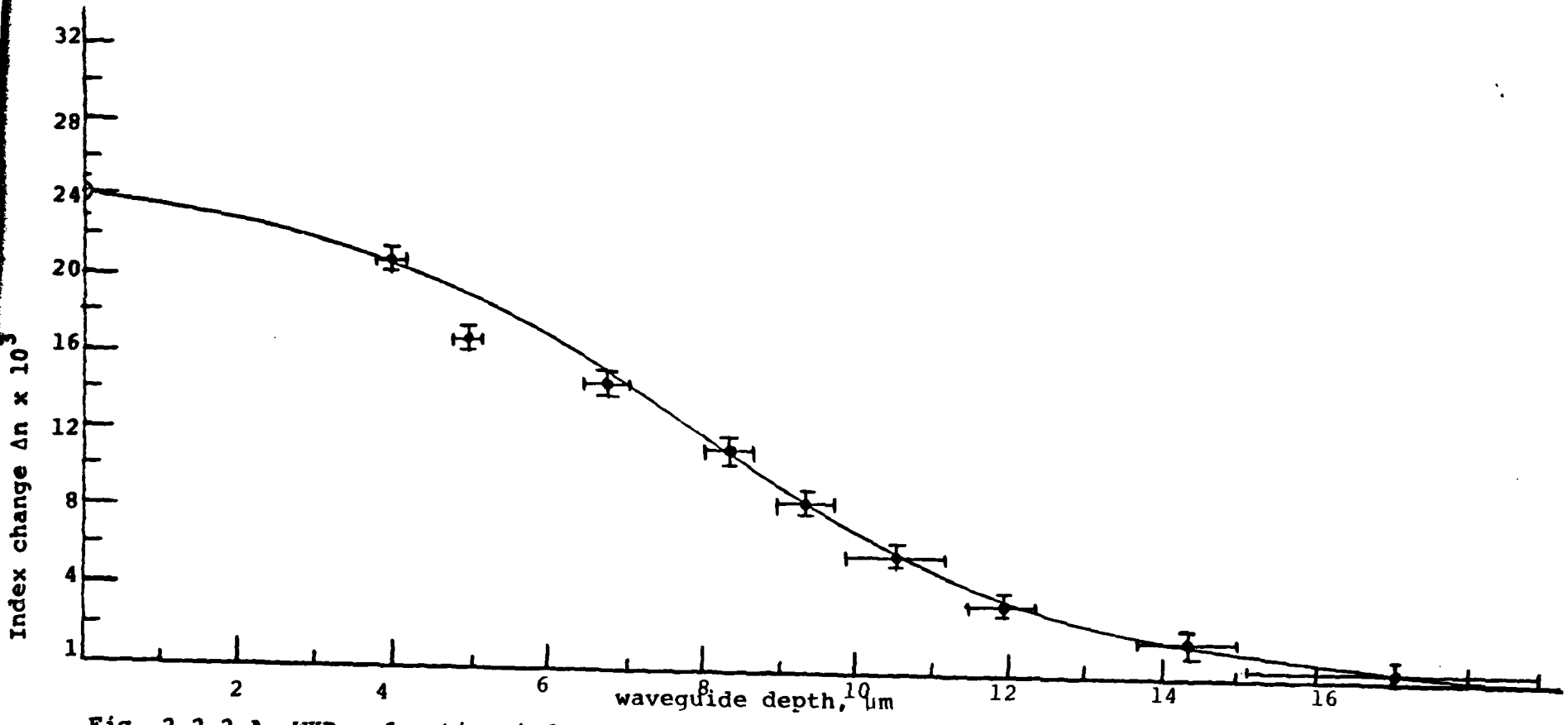

Fig. 2.2.2.A WKB refractive index profile for waveguide fabricated in S3 glass by field assisted diffusion at 400°C with an electric field of 40 V/mm applied for 15 min.

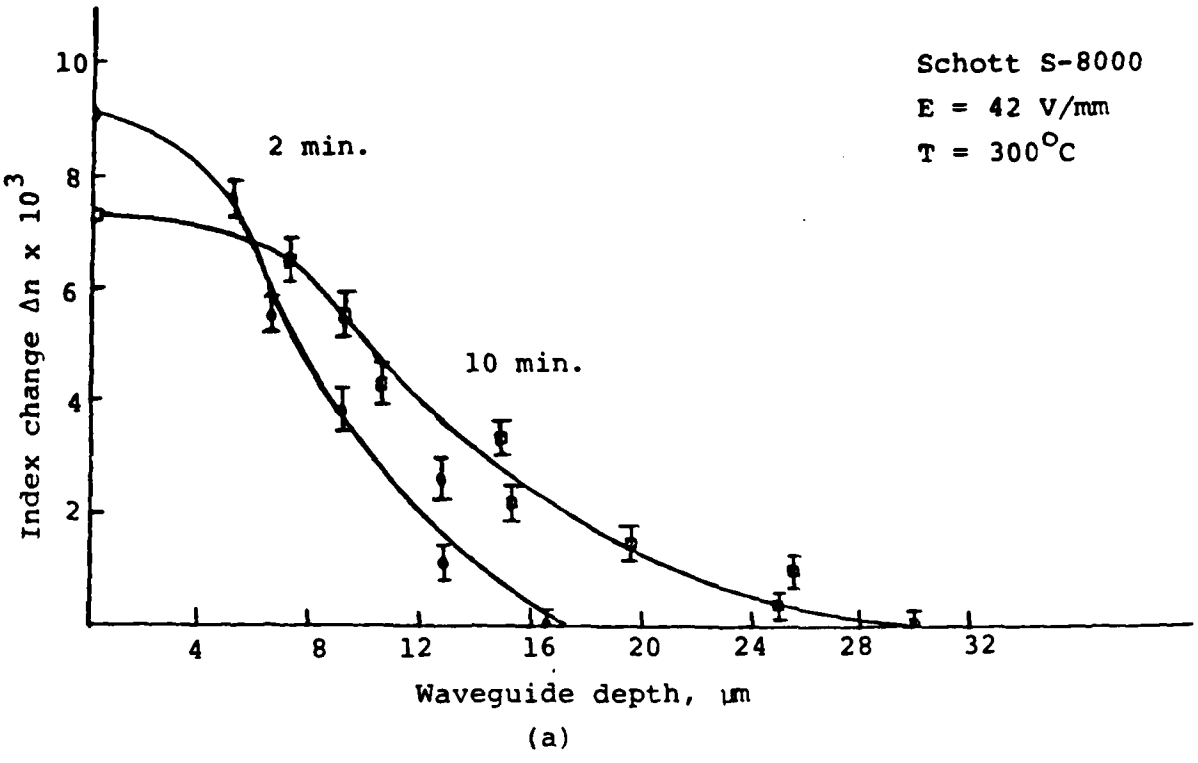

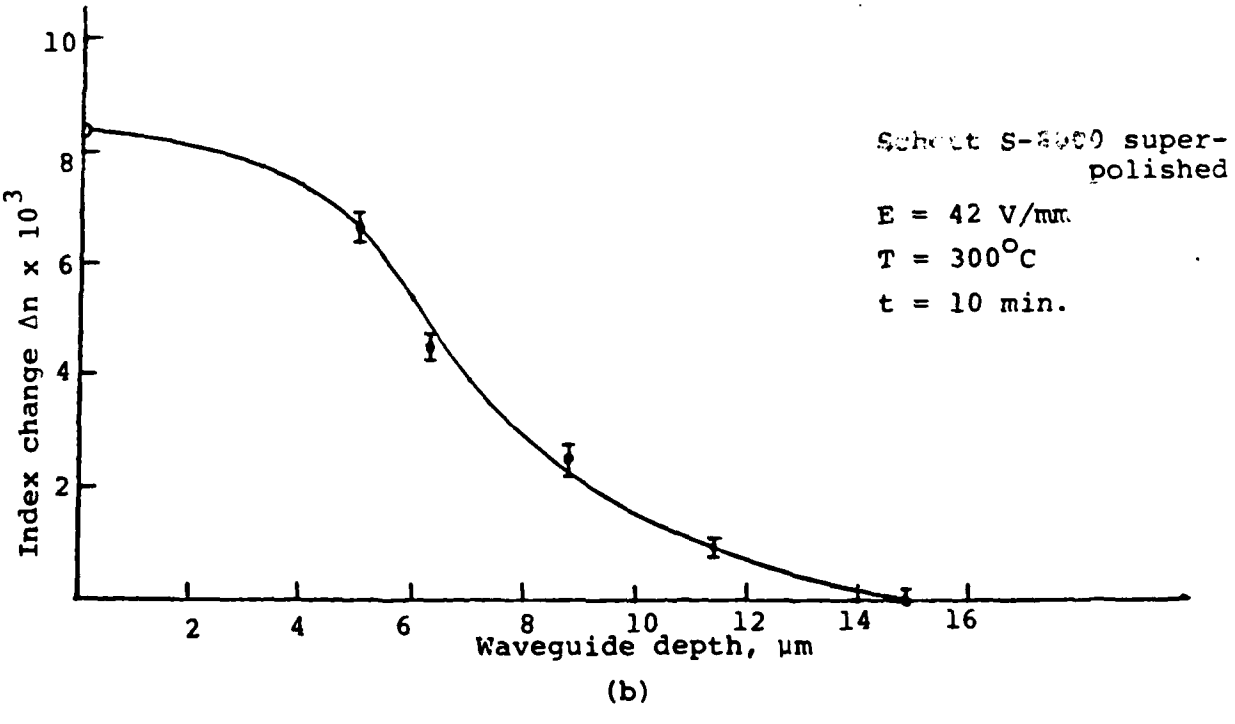

Fig. 2.2.2.B WKB refractive index profiles for electric-field assisted diffusion in Schott S-8000. The difference in the two curves in (a) shows that the silver at the surface was being depleted during the 10 min. diffusion. Field-assisted diffusion in the super polished sample shows an increase in Δn with a corresponding reduction both in the number of modes and the depth of the guide.

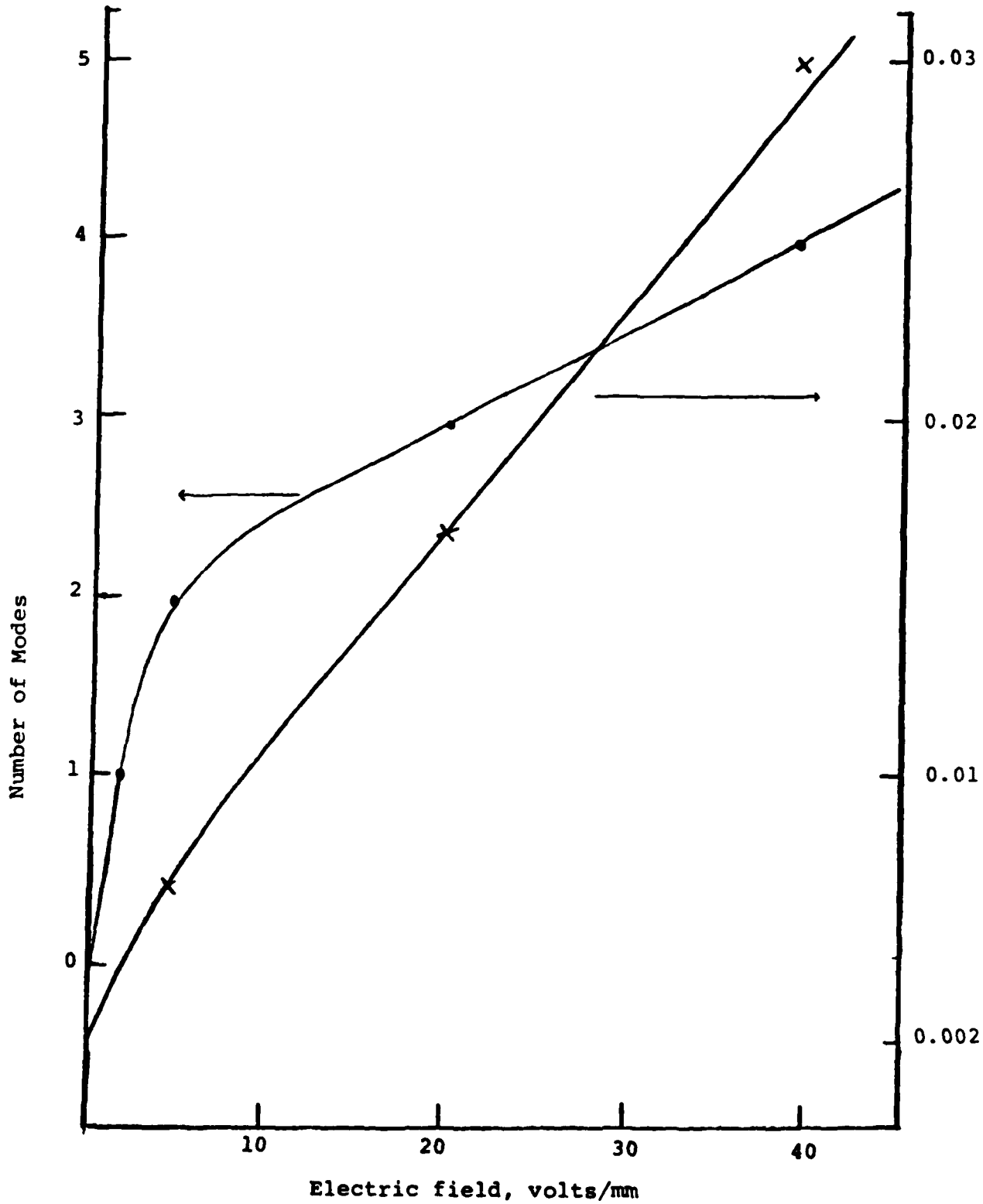

Fig. 2.2.2.C Dependence of Δn and mode number on applied field during diffusion.

field back to zero field, it is possible to estimate Δn for the single mode guide fabricated with a field = 2V/mm. This value is given in brackets in the table. The value of Δn at zero field was determined approximately by extrapolating results for thermal diffusion at higher temperatures back to lower temperatures and shorter times. Figure 2.2.2.D shows the refractive index profiles for these waveguides.

We performed loss measurements on waveguides fabricated in both optical glasses. Our results with these glasses show that when gold electrodes were used, the waveguides fabricated by field-assisted diffusion exhibited a great deal of in-plane scatter and were significantly more lossy than those fabricated without an applied electric field. The mode-dependent losses are shown in Figs. 2.2.2.E and 2.2.2.F.

To reduce the losses introduced by this fabrication step we did field assisted diffusion without the gold anode, using only the silver film as a contact. The gold cathode, which does not affect the guiding surface, was retained. Fig. 2.2.2.F shows that with this technique the losses with field assisted diffusion are reduced by a factor of 6. We also observed a significant reduction in in-plane scatter in these guides. A possible explanation for the large losses observed when a gold anode is used is that gold migrates into the guiding layer during the diffusion and causes an increase in scattering in the waveguide. We intend to use only silver anodes in the future.

The increase in loss with mode number seen in Figs. 2.2.2.E and 2.2.2.F indicate that the losses are limited by surface rather than by volume loss mechanisms. Both surface and volume losses increase as the waveguide thickness decreases. Thus thinner guides are always more lossy. Typically waveguide loss is inversely proportional to waveguide thickness. The increased losses in waveguides fabricated by field assisted diffusion are due to the fact that they are thinner. Under the diffusion conditions ($T = 350^{\circ}C$ $E = 20V/mm$ $t = 15$ mins) waveguides

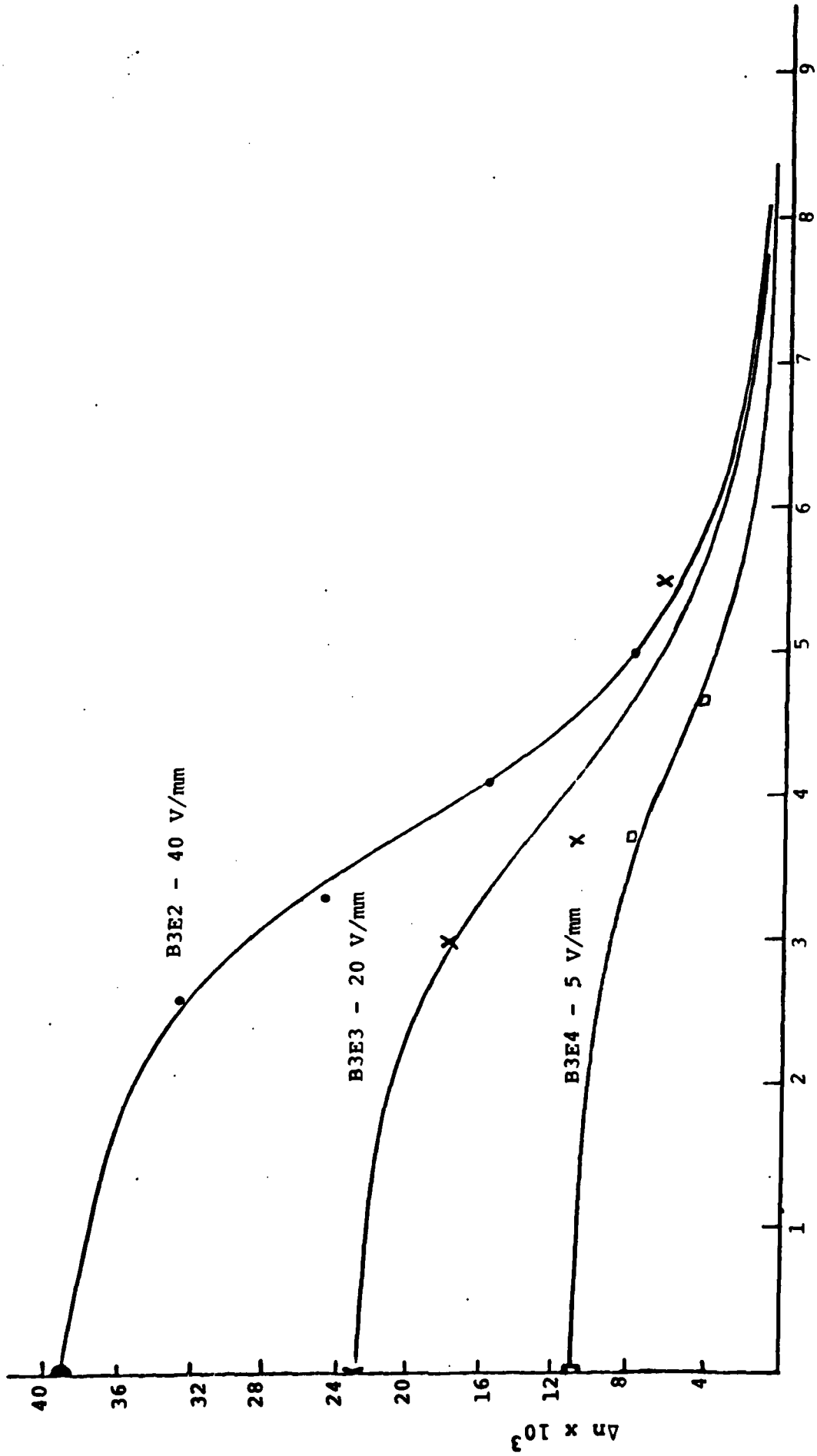

Fig. 2.2.2.D Index profile for guides fabricated at 350°C with electric field applied for 15 min.

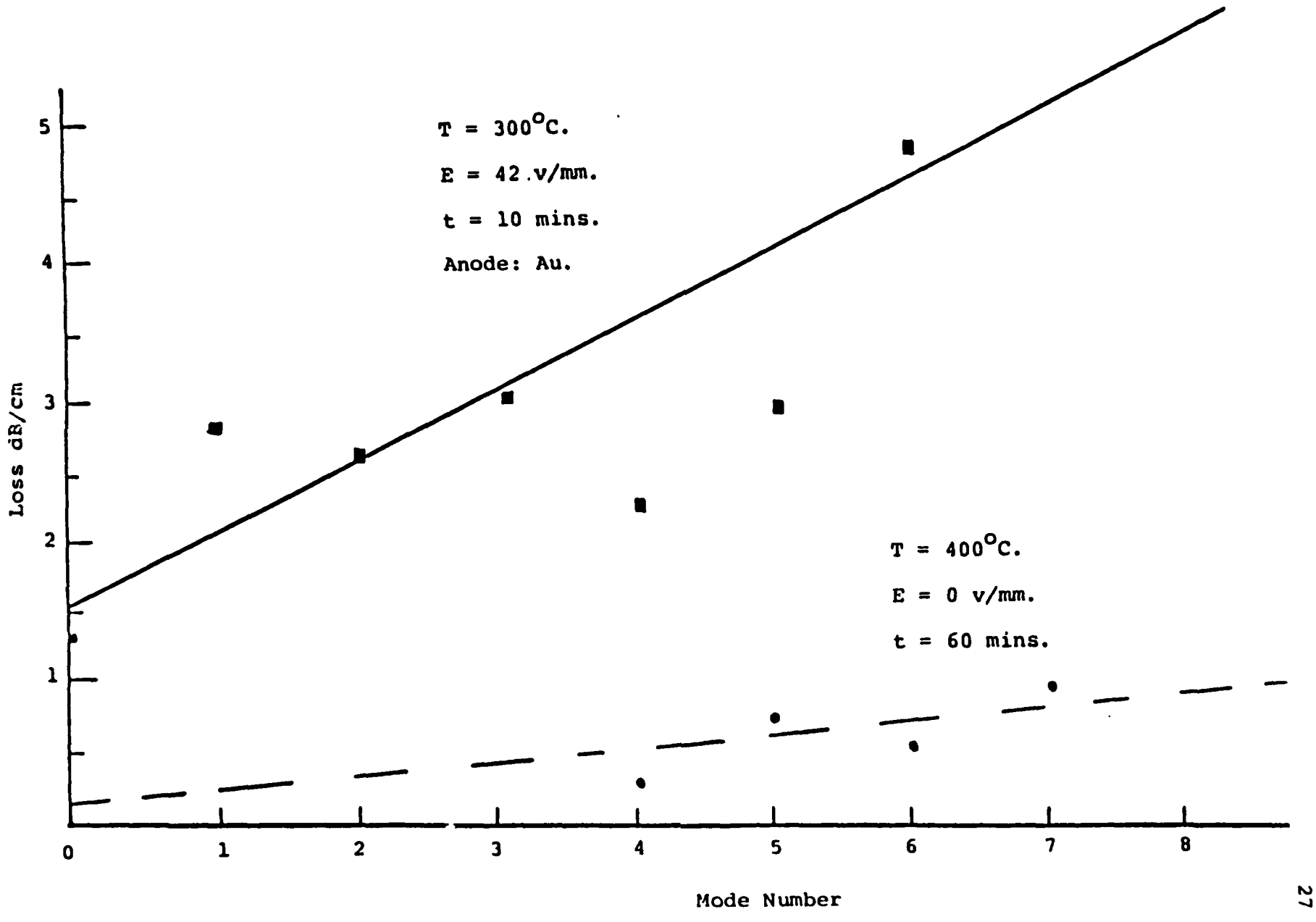

Fig. 2.2.2.E Mode dependence of the losses in waveguides fabricated in S-8000 glass with and without an applied electric field.

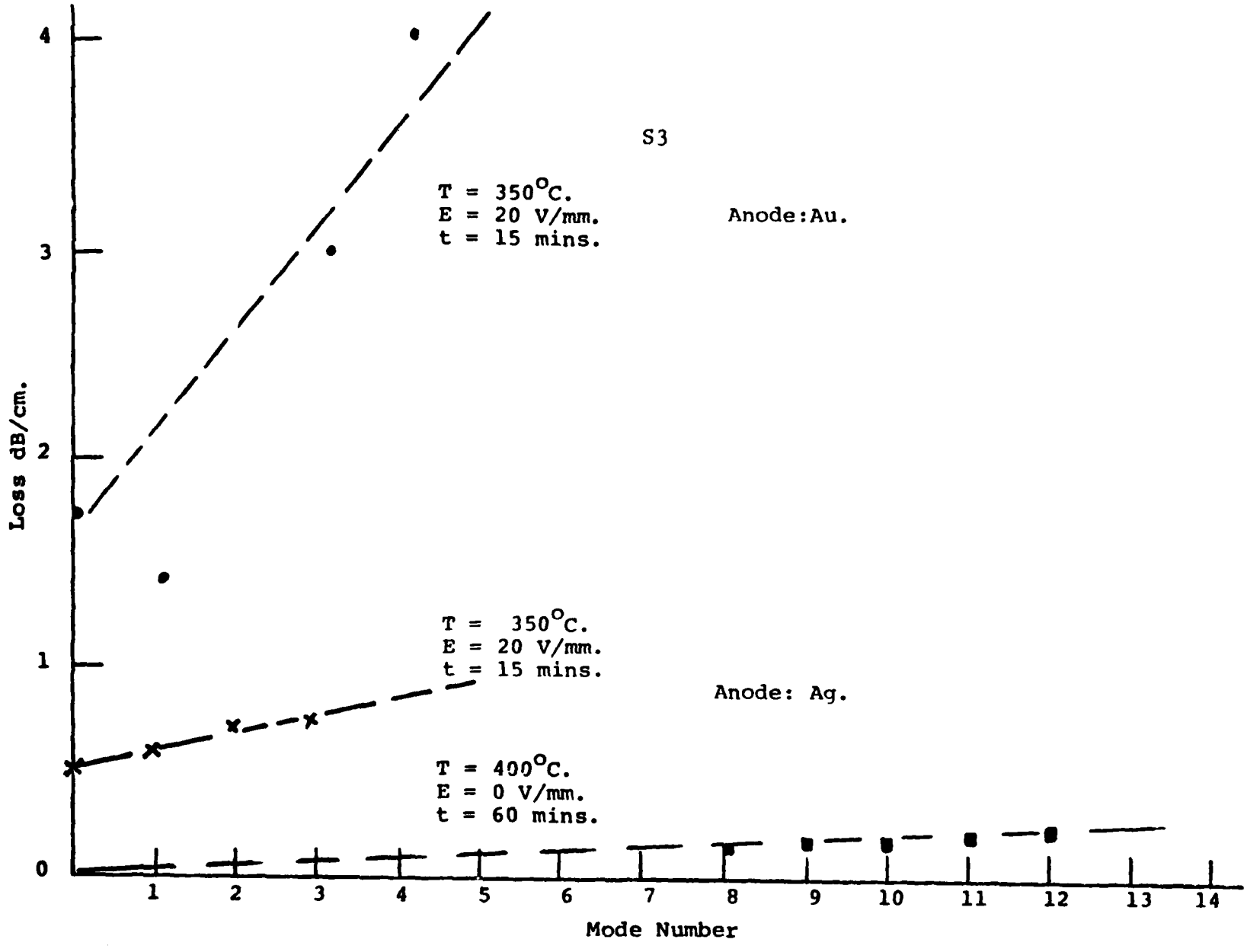

Fig. 2.2.2.F Mode dependence of the losses in waveguides fabricated with and without an applied electric field.

fabricated by field assisted diffusion are approximately 8 μm thick as opposed to the 50 μm - 60 μm thickness of guides fabricated without an electric field(Fig. 2.2.1A). Hence a loss of 0.5 dB/cm in a 8 μm thick guide would correspond to a 0.1 dB/cm loss in a 50 μm thick waveguide. This is comparable to the average loss measured in the 50 μm thick waveguides (Fig. 2.2.2.F; T = 400°C, E = 0, t = 60 mins), showing that the addition of an electric field did not introduce a new loss mechanism.

The ultimate source of loss is apparently scatter from surface roughness. The scatter can be seen both by observation of the streak of guided light and in scattering between guided modes. We have seen a strong reduction in loss when we coat the surface with methanol.

We are pursuing burying the guide to eliminate these residual losses. We are also investigating index match liquids to reduce the surface scatter.

2.2.3 Laser Writing of Narrow Lines and Parallel Channels

At the time of the final report last year we reported our success in using laser writing to define channels in photoresist, both straight and curved. During this present contract we have extended these studies to etching channels in silver using the photoresist masks. In order to obtain uniform and narrow channels, it was found necessary to dilute the etch solution with 10 parts water. Photographs of three silver channels ranging in width from 4 μm to 20 μm are shown in Fig. 2.2.3.A. These pictures were taken directly after the etching step and the dark patches seen are silver oxide residue not removed by the etchant.

Directional couplers with separations ranging from 4 μm to 10 μm fabricated by our laser writing technique are shown in Fig. 2.2.3.A also. A Twyman-Green interferometer included in our experimental arrangement provides the capability of writing channels separated by fractions of a wavelength. The experimental arrangement for the laser writing including the interferometer, is shown in Fig. 2.2.3.B. The interferometer consists of a fixed mirror M1 and a mirror M2 attached to the motor-driven translational stage on which the sample is mounted. The reflected beams from M1 and M2 are superimposed and the resulting fringe pattern is magnified and projected onto a screen, S. As the translation stage moves, the changing optical path length makes the fringes appear to move across the screen. This fringe motion is seen by a detector positioned behind a pinhole in the screen and recorded by a strip chart recorder. Since the passage of one fringe corresponds to a change in optical path length equal to the wavelength of the probe we can in principle write lines separated by a fraction of a wavelength (λ = 0.46 μm).

Figure 2.2.3.Ad shows four channels, separated by 10, 4 and 7 micrometers fabricated by using the interferometer. The apparent breaks in the second exposed channel are due to vibration of the microscope objective, and have been eliminated in recent experiments by the use of more stable mounting hardware for the optics.

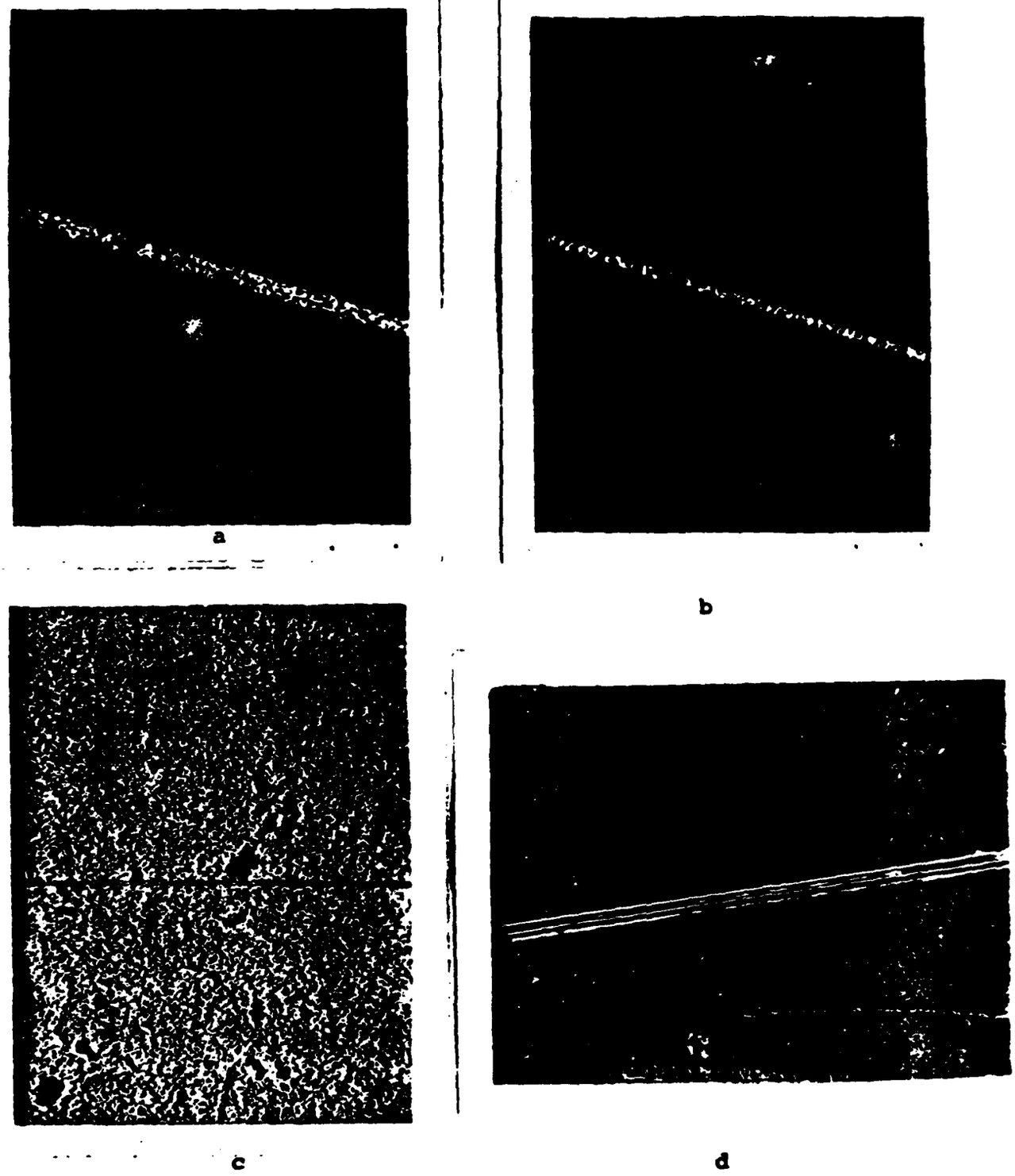

Fig. 2.2.3.A Silver channels (a) 20 μm (b) 13 μm (c) 4 μm wide fabricated by varying the writing speed during laser lithography. (d) directional couplers separated by 10, 4 and 7 μm obtained using the Twyman-Green interferometer arrangement.

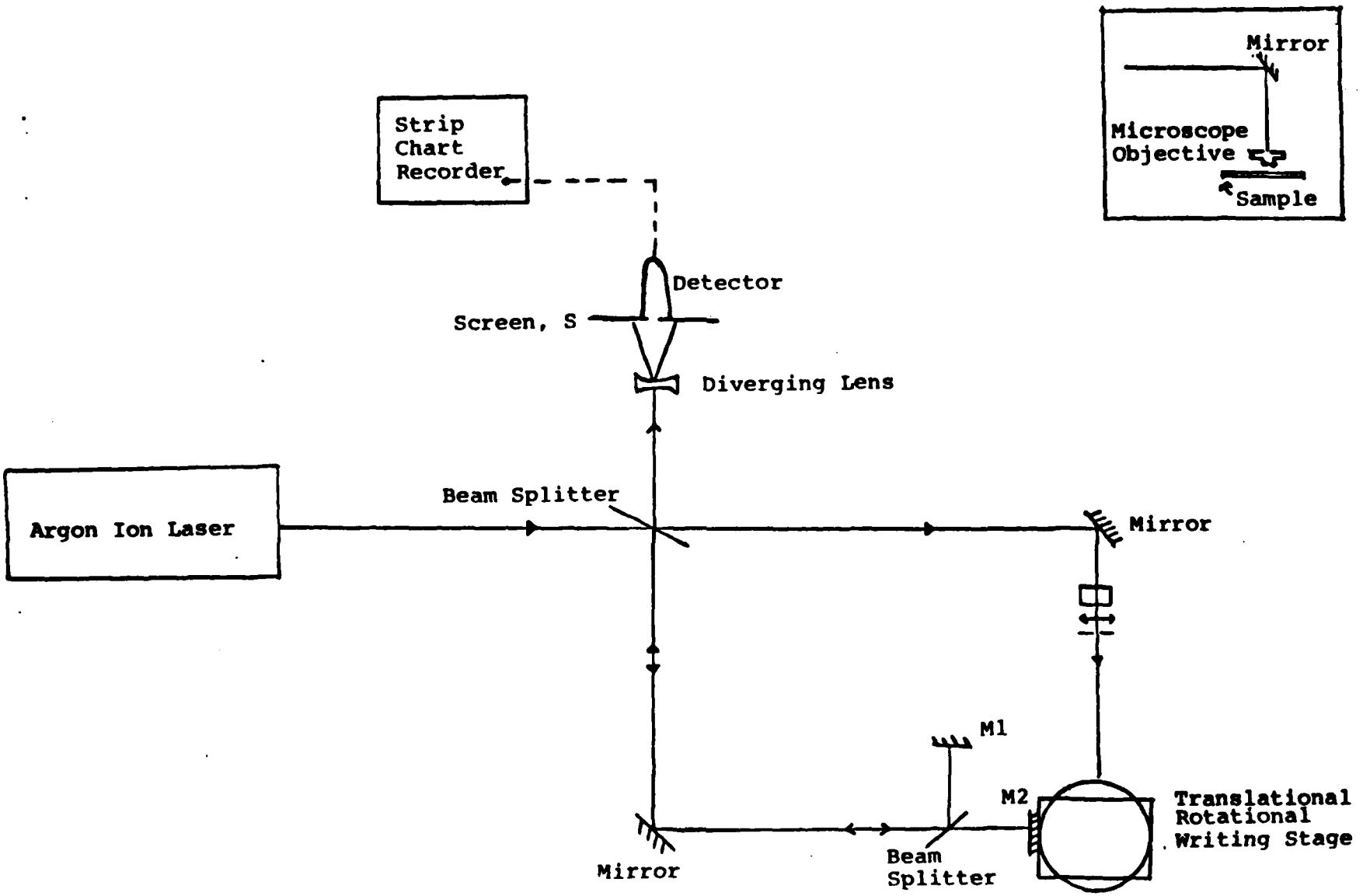

Fig. 2.2.3.B Experimental arrangement for writing directional couplers and narrow channel waveguides. The Twyman Green Interferometer consists of two orthogonally positoned mirrors M1 and M2. The detector monitors the motion of the interference fringes across the screen. The circle indicates the position of the beam turning mirror and focusing objective shown in the insert.

2.2.4 Laser Writing of Masks

Because of the difficulties of obtaining channel stripes in silver without breaks reported in section 2.2.3, we decided to use the laser beam to write masks, which would then be replicated onto the substrates by standard photolithographic techniques, using our mask aligner. This research effort was very successful, and culminated in a paper which will be in the special issue on techniques for the Fabrication of Integrated Optical Circuits, published by the IEEE Transactions on Fabrication for Integrated Circuits, with authors Wilson, Mueller and Garmire. The preprint follows:

Abstract

Masks for integrated optics applications have been fabricated using a focused Argon laser beam to expose a photoresist-coated gold-chrome plate. Curved and straight line masks were written using a combination or precision motor-driven rotational and translational stages to move the coated plate under the focused laser beam. By varying the laser power and/or writing speed, we have made directional coupler masks 3 μm wide separated by as little as 1 μm. Our results show that narrow lines several centimeters long with better than 1000Å edge roughness can be obtained by this fabrication technique.

Guided wave devices, unlike conventional electronic devices, often require small dimensions on the order of microns in one direction and large dimensions on the order of centimeters in the perpendicular direction. Conventional photolithographic techniques such as electron beam writing and pattern generation methods have been shown to produce the high quality masking structures (200Å edge roughness) [1] which are required in integrated optics. However, these techniques require some sort of "step, align and repeat" procedure, often causing abrupt irregularities. In addition to the long lead time to delivery, these masks are expensive and fabrication of complex designs can rapidly deplete the resources of a modest research grant. The research scientist must therefore either deal with simple structures or find an alternative means of fabrication. Laser writing offers such an alternative. We have been exploring the possibilities of laser writing of masks for applications which require long waveguides only a few microns wide. In particular, we are working on a development of a ring interferometer in glass, consisting of a ring waveguide 10 cm diameter and directional couplers for input and output coupling. The apparatus shown in Fig. 1 has been designed for this purpose.

A combination of neutral density filters and polarizers were used to vary the laser power, and the patterns were written by using precision motor driven translational and rotational stages to move the mask under the focused laser beam. By changing the distance from the axis of rotation to the position of the focused beam, we were able to vary the radius of rings and the curvature of circular sec-

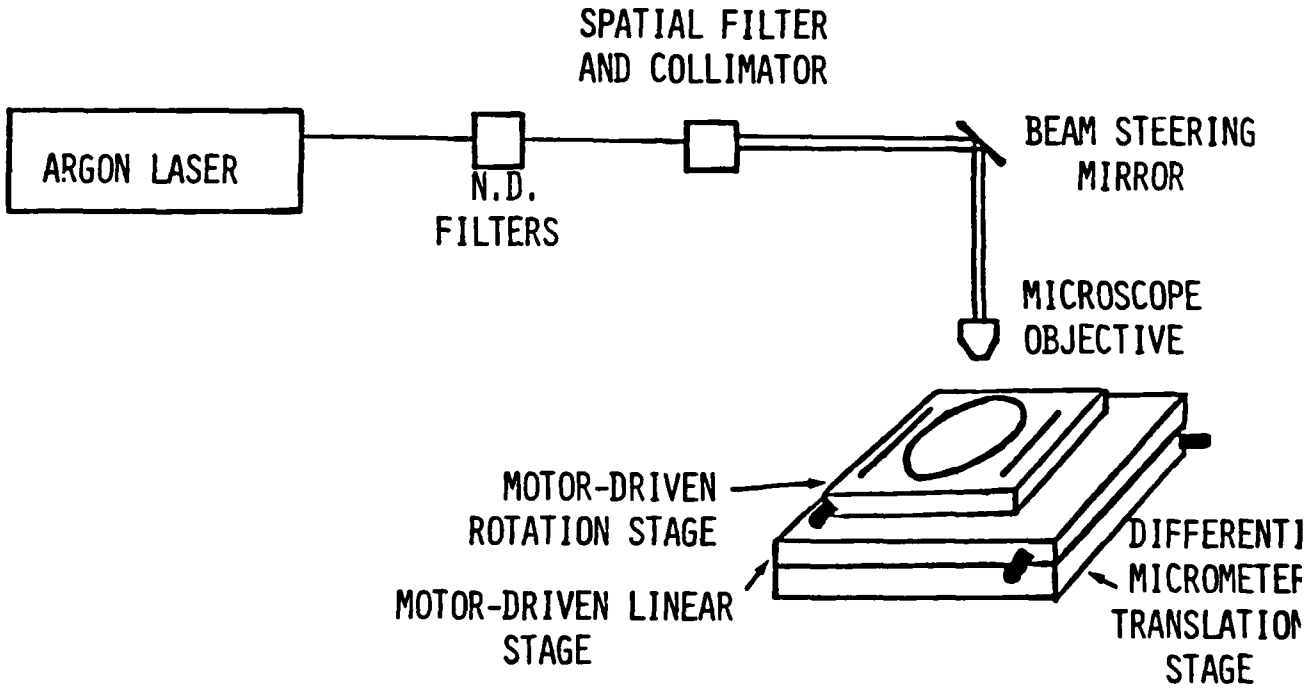

Fig. 1 Experimental arrangement for laser writing of masks.

tions. Directional couplers were fabricated by laterally translating the mask a few micrometers before writing the next pattern. The lateral motion of the stage was monitored using a Twyman-Green interferometer, one arm of which consisted of a reflector mounted on the translational stage. By recording the motion of the interference fringes resulting from the change in optical path length, we were able to determine accurately the center to center separation between two adjacent lines. Vibrational isolation was achieved by mounting the entire system on an air suspension optical table.

Masks suitable for contact printing were fabricated using a standard gold-chrome mask coated with a thin layer (5000Å) of positive photoresist (AZ 1350J). Although the optimum operating range for this resist is around 350 nanometers, we have found it to be sufficiently sensitive at the short Argon laser wavelengths (4545Å and 4579Å) to obtain good patterns when operating at microwatt laser powers. Using the 4545Å Argon wavelength, we have written lines as small as 2.5 micrometers wide which is on the order of the diffraction limited spot size. In this paper we demonstrate some of the structures which laser writing can produce and indicate some of the fabrication limits of the process.

Typical laser powers for laser writing range from 8 μW to 0.5 mW with writing speeds varying from 0.3 to 3 mm/sec. Making use of the laser beam's Gaussian intensity profile to control the linewidth, lines range in width from 2 μm to 24 μm have been produced by adjusting both the laser power and translation rate. Alternatively, the linewidth can be varied by defocusing the laser beam or by using a different microscope objective. The two parameters which

determine the precision to which the writing stage must be aligned are the focused spot size and the depth of focus. For a Gaussian beam, the minimum spot size is given by $1.3 \lambda f/d$

where λ is the wavelength, f is the focal length of the objective lens and d is the beam diameter. [2]. For a 2 mm beam diameter and a 20X microscope objective, the calculated minimum spot size (separation of $1/e^2$ power points) is 2.3 μm. With this microsccpe objective and a translational speed of 0.3 mm/sec, 4 μm and 7 μm wide lines have been written at laser powers of 40 μW and 80 μW, respectively, (Fig. 2). The depth of focus for a Gaussian beam is given by $\pm$ 2.5 $\lambda (f/d)^2$. The calculated depth of focus for our arrangement was $\pm$ 18 μm. Thus the focused spot size did not change significantly within the 0.5 μm thick photoresist layer. However, to obtain lines of uniform width over long distances, optical alignment of the translational stage over the length of the beam travel is crucial. This was achieved by ensuring that reflected and incident beams remained collinear over the length of the travel of the stage. With this alignment procedure, we were able to write lines 4 μm wide over a 6 cm length.

A typical line drawn by laser writing is shown in Fig. 3. Notice that the edges are sharp. However, there is approximately 1000Å residual edge roughness of about 6 μm periodicty along the

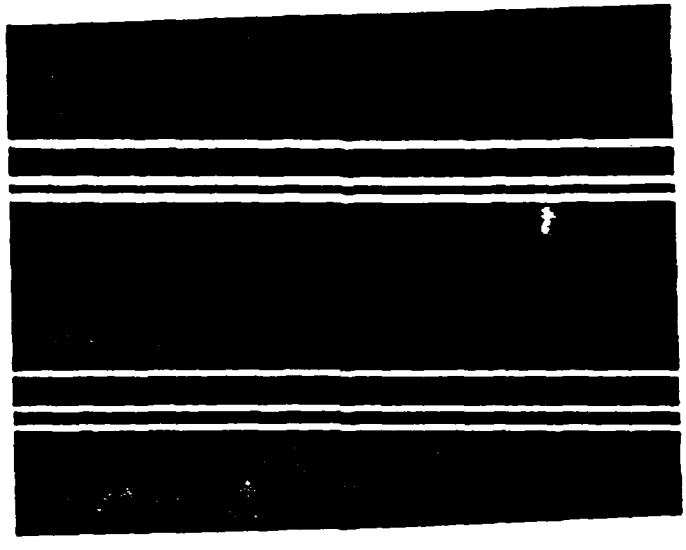

Fig. 2 256X magnification of mask for parallel lines fabricated by laser writing. The lines 4 μm (lower group) and 7 μm (upper group) wide were written using 40 μW and 80 μW of laser power, respectively.

Fig. 3 1200X magnification of 6 μm wide lines showing a 6 μm period in edge roughness.

length of the line. Possible mechanisms for the residual edge roughness are fluctuations in laser power, deviations of the translation stage, vibrations in the system and photoresist processing limitations. To determine the cause of the edge roughness, we compared the lines drawn by using the rotational and translational stages. The arcs written with the rotational stage were of very high quality with no edge roughness measurable at 1200X magnification. An example is shown in the top channel of Fig. 4. In comparison the line drawn using the translational stage (bottom channel in Fig. 4) does exhibit 0.1 μm residual edge roughness. This indicated that random variations such as fluctuations in laser power and system vibrations were not the cause of the observed edge roughness but instead it was due to a slight wobble in the translation stage. In addition to the edge roughness, the edge of the bottom lines show the effects of incomplete development. However, edge sharpness can be enhanced by optimizing the exposure so that the photoresist channel edge occurs at the half power point of the focused Gaussian beam.

Directional couplers can be made by combining an arc and a straight line (or two arcs), separated by a small distance. For this purpose we wrote arcs of 40 cm radius of curvature, of width 3 μm and length 5 cm. We also wrote a ring waveguide, 7 cm in diameter with a linewidth of 15 μm. This ring will form the basis for a ring interferometer. To further explore the potential of laser writing for directional couplers, we wrote several lines using the translation stage and varying th separation

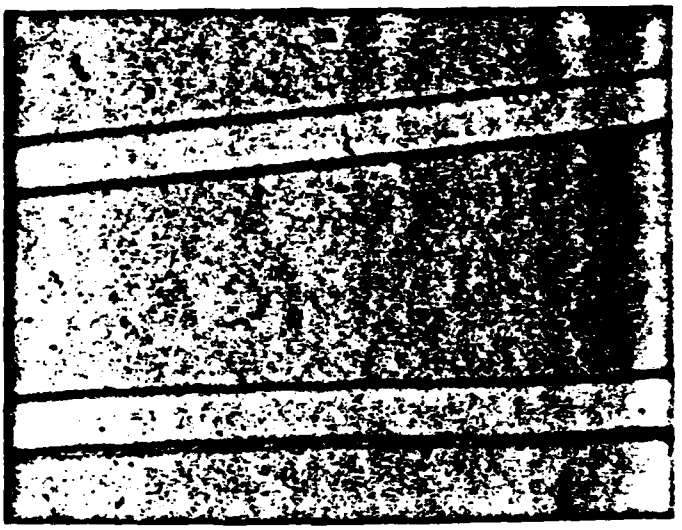

Fig. 4 Pre-etch photographs of lines written with the rotational stage (top) and the translational stage (bottom). Notice that there is no wobble present in the top trace even at this 1200X magnification.

between the lines. One such pattern is shown in Fig. 5. The lines are 2.5 μm wide with 1.5 μm edge to edge separation. For this exposure, the separation between these lines was controlled by a differential screw translator which had a resolution of 0.125 μm. The results obtained using the differential translator are similar to those obtained with the Twyman-Green interferometer. Other structures written by laser writing are the crossed and Y power splitters shown in Figs. 6a and 6b.

We found it difficult to align our setup sufficiently accurately to write both an arc and a straight line separated by the required spacing for a directional coupler. More typically, the two lines would intersect. For this reason we have found it most convenient to write a master arc and straight line, and to contact print both onto another mask, carefully adjusting the spacing under a microscope.

We have fabricated both glass and $LiNbO_3$ waveguides, single and multimode, using these masks. We have not made careful comparison of waveguides made with these masks and those made by e-beam written masks, but are confident that the laser-written masks compare favorably. We are now using laser-written masks for all our optical circuits.

Fig. 5 640X magnification of directional coupler mask written by laser writing. The lines are 2.5 μm wide and separated by 1.5 μm.

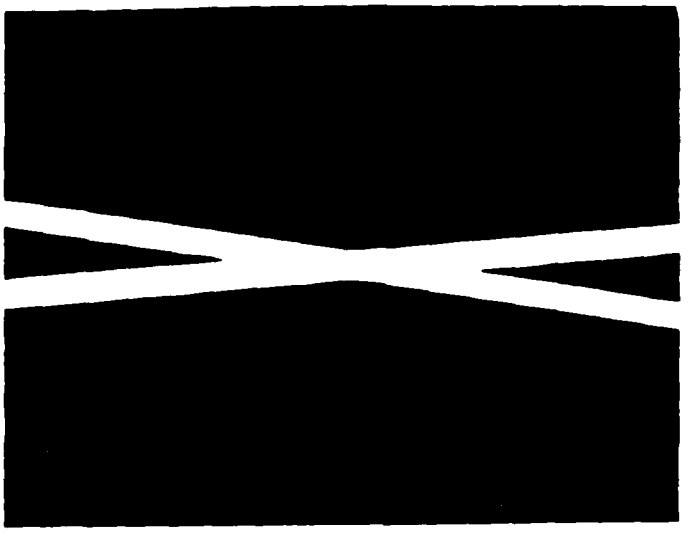

(a)

(b)

Fig. 6 Illustrated are masks for crossed (a) and y (b) power splitters under 256X magnification. The lines are 16 μm wide in (a) and 6 μm and 8 μm wide in (b).

In conclusion, we have demonstrated some of the capabilities of laser writing as a tool for fabricating masks for integrated optics circuits. We believe that the potential advantages of this technique are sufficient to make it a viable option to existing methods. One possible extension of the technique would be to use a computer controlled X-Y stage to fabricate arbitrary mask structures. In the meantime, we have found the combination of one translation and one rotation stage gives enough flexibility for several applications.

References

1. M. Barnoski, Introduction to Integrated Optics, Plenum Press, New York, 1974, p. 178.

2. A Yariv, Quantum Electronics, Wiley, New York, 1975, p. 117

3. J. Haavisto, G. A. Pajer "Resonance Effects in Low-loss Ring Waveguides" Optics Letters 5 510 (1980)

2.2.5 Groove/ridge formation in field assisted diffusion

It was discovered in November that narrow channel waveguides fabricated in microscope slides had surfaces which were depressed, relative to the surrounding substrate, causing grooves. Preliminary data was described in section 2.1. Further experimentation continued to provide inconsistent results since some substrates, under some conditions, produced ridges rather than grooves. We have made some preliminary measurements of height variations in waveguide surfaces which are outlined in Table 2.2.4. It should be noticed that field-assisted diffusion at high temperatures leads to groove formation, while diffusion at lower temperatures generally results in ridges, rather than grooves. Furthermore, no height-dependent effects are seen when no electric field is applied.

Since part of the unreproducibility is undoubtedly due to the unreproducibility of microscope slides, we have begun study of groove/ridge formation in S2 and S8000 glass. Preliminary results indicate that S3 has grooves, while S8000 has ridges, proving that glass composition is important in determining whether the glass shrinks or expands during silver diffusion.

It is not our intention to pursue this subject exhaustively. However, groove formation has hindered our ability to see waveguiding in narrow waveguides since it raises the prism above the waveguide. This is not an insurmountable problem, however, because channel waveguides can be conveniently excited with end-coupling, so that prism coupling is not a required technique. It does mean, however, that the edges of the glass substrates must be polished before waveguiding can be observed. This proved to be a time-consuming limitation, and we were not able to observe 4μm channel waveguides in glass before the contract ended.

Sample	Field V/mm	Temperature °C	Time min.	Channel Width μm	Height Change Å	Number of Modes
DC1	90	400	210	15	-3500	--
DC2	100	400	36	15	-2000	--
DC3	100	300	18	15	- 500	--
DC4	100	350	7	15	-4000	--
KST1	30	300	17	500	+ 500	--
KST7	10	300	6	500	+ 400	--
KST8	10	300	6	500	+ 450	--
319	10	300	10	500	+ 150	--
320	40	300	10	500	+ 175	--
325	60	300	10	500	+ 250	--
327	100	300	10	500	+ 200	--
331	100	300	30	500	+ 280	6
S8-4	42	300	10	step	+7000	6
anode					-2000	
S8-B7 4/7 (superpolish)	42	300	10	step	0	4
S3 - BE1	40	400	15	step	- 300	--
anode					+ 250	

Table 2.2.4 Height change (+ for ridge, - for groove) for a number of diffusion conditions and glass substrates

3. ADDITIONAL RESULTS

3.1 Photoacoustic Measurement of Refractive Index Profile in Glass Waveguides

3.1.1. Introduction

Photoacoustic measurements provide a method of indirectly measuring the refractive index profile in glass waveguides. This technique therefore allows an independent verification of index profile measurements made using the conventional prism coupling method.

The waveguides under study were fabricated by electric-field-aided thermal diffusion of silver into a glass substrate. Since the induced changes in refractive index and optical absorption coefficient are both proportional to the silver ion concentration, the absorption profile provides the index profile. Absolute calibration can be obtained using a sample fabricated to have a uniform silver ion concentration throughout, and on which bulk measurements of refractive index and absorption coefficient have been made.

This was the abstract of a paper presented at the Second International Topical Meeting on Photoacoustic Spectroscopy, Berkeley, CA, June 1981 by K. Cheng, R. Swimm and P. Yeung).

3.1.2. Results

Measurements were taken to determine the Ag^+ depth profile in a planar glass waveguide using the depth profiling capability of photoacoustics. This capability results from the fact that the PAS signal is due only to the light absorbed in a layer extending from the surface of the sample down to a depth which is determined by the chopping frequency of the incident light.

Measurements were made by using a glass waveguide as the back window of the cylindrical cavity in the photoacoustic cell (Fig. 3.2A). Chopped laser light illuminated the waveguide normal to the surface. In this configuration, the waveguide did not guide the light, but merely acted as an inhomogenous sample with an absorption coefficient which varied as a function of depth. Violet light was used for the measurement in order that the waveguide would absorb strongly compared to the undoped glass substrate and hence respective contribution from each could be separated. Absorption in the waveguide layer was predominantly due to Ag^+, but not to colloidal Ag, which merely scatters light.

The photoacoustic signal arises when heat due to absorption of the laser beam in the sample diffuses to the surface of the sample where it heats the air in the PAS cell cavity. Since the light is chopped, the air in the cell alternately heats and cools, which results in a pressure variation which is sensed by a microphone in the wall of the PAS cell. This signal is then measured using a lock-in analyzer. In this way, signals as weak as 10 nvolts were measured.

The measurement procedure consisted of two steps. In the first, the magnitude and phase response of the system were calibrated by measuring a sample of known properties.

Once the system response characteristics were determined, the glass waveguide was measured. The magnitude and phase data are shown in figs. 3.2B&C. The magnitude data behaved as expected. The deviation away from ω^{-1} behavior at low frequency is due to substrate absorption, and may provide a means of calibrating the absolute absorption in the waveguide if substrate absorption is known. The deviation at high frequency is a result of the finite depth of the waveguide, and in principle provides depth profile information.

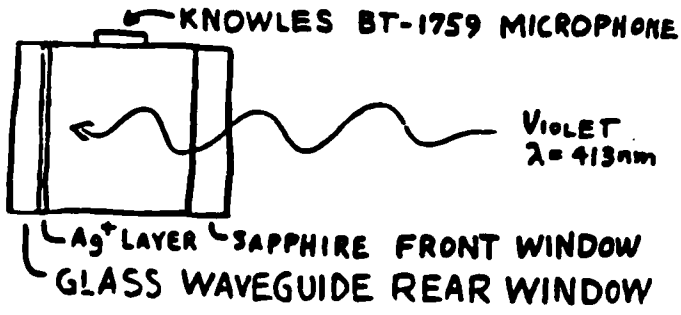

Fig 3.2A - PAS Cell Geometry

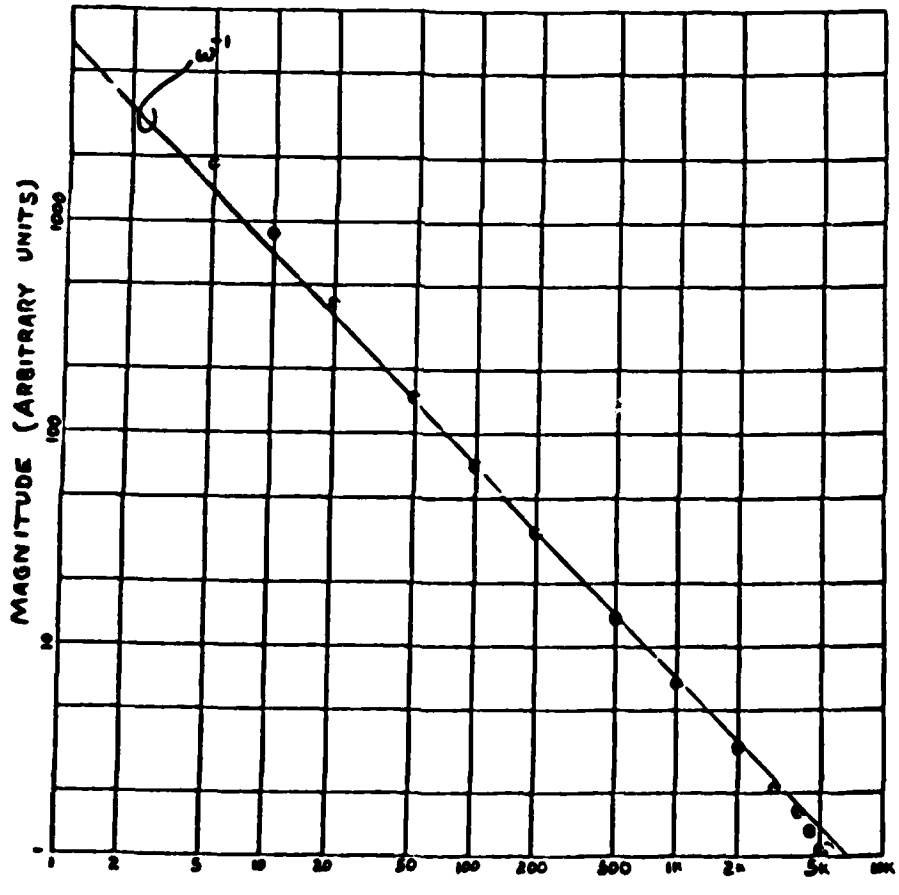

Fig 3.2B - PAS Magnitude vs. Frequency for Glass Waveguide

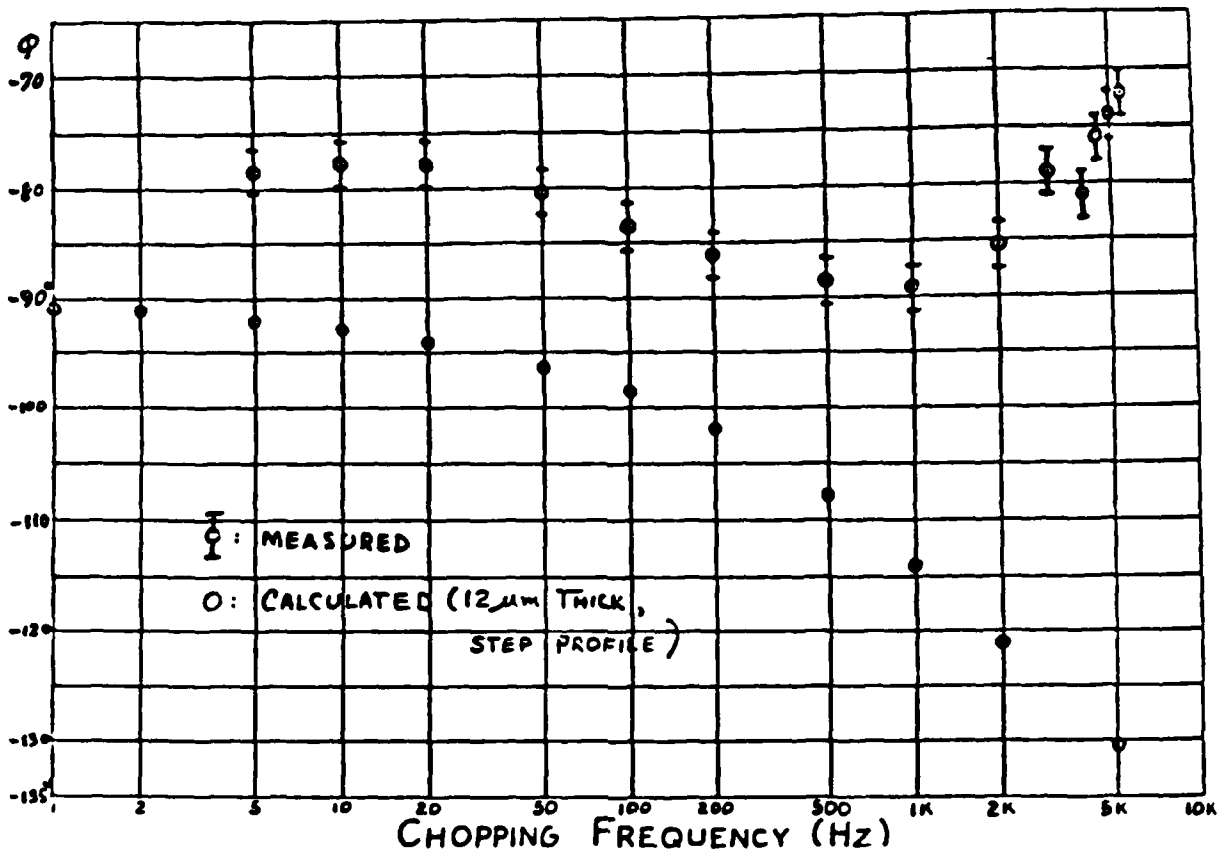

FIG. 3.2C - PAS PHASE VS. FREQUENCY FOR GLASS WAVEGUIDE

However, because of the relatively weak dependence of the magnitude on the absorbing layer thickness (i.e. waveguide depth) it is well known that the magnitude data is unsuitable for depth profiling. The phase, on the other hand, is a strong function of the waveguide depth, and for sufficiently wide chopping frequency variation can also provide the depth profile accurately.

Fig. 3.2.C shows preliminary phase data, as well as model predictions. The model calculations were for a step profile, 12μm deep. The actual diffusion profile is, of course, not a step. Conventional prism coupling measurements show a guide depth of ~4μm for the deepest guide mode. The diffused layer is expected to extend somewhat deeper than this. Also, uncertainties in the thermal conductivity of the waveguide layer make the length scale in a PAS depth profile correspondingly uncertain, as discussed below. Nevertheless, the general agreement of the data below 500 Hz, and the fact that the PAS measurement yields a plausible guide thickness indicates that the waveguide has been successfully detected.

Deviations of the data at high chopping frequency are believed due to flexing of the waveguide in a drumhead mode. This will be investigated, and should be easily corrected through cell modification. The slight down-turn of the data at low frequency was consistent wi the onset of substrate contributions as indicated in the magnitude data. The 15^{o} offset between the measured and predicted results is not understood at this time. Calibration will be rechecked to verify its validity. In addition, there are various systematic effects which are still under investigation by workers in the photoacoustic community. Finally, in comparing the measured data with the model predictions the effect of alterations of the thermal conductivity of the glass by the introduction of Ag^{+} must be considered. Since the depth information is obtained via a time measurement (i.e. since the phase delay depends on the thermal conductivity of the sample), the thermal properties of the sample must be understood. Various operating modes of the photoacoustic technique provide an excellent way to determine these thermal properties. The data obtained to date demonstrate that depth profile information can be obtained with currently available methods. Once the required corrections to the data are determined, the phase variation can provide the depth profile using the method of Afromowitz et.al.[2]

References

1. A. Rosencwaig, Second International Topical Meeting on Photoacoustic Spectroscopy Technical Digest, ThA2-1 (1981).
2. M. A. Afromowitz, P. S. Yeh and S. Yee, J. Appl. Phys. 48, 209 (1977).

3.2 Attempts to Diffuse Waveguides into Quartz

Most processes which introduce waveguides into glasses use diffusion of silver ions, which typically takes place by exchange with sodium ions. Last year we attempted to fabricate waveguides in phosphate glass which contained no sodium, and found that no waveguides were formed; apparently the silver would not enter without the presence of sodium. However, we decided to look for waveguide formation in quartz anyway, just in case. We made two attempts to fabricate waveguides in ULE by diffusion of silver. These experiments were performed by both thermal and electric field-assisted diffusion from evaporated silver films.

In the first experiment the samples were placed in the furnace at 500°C in a flowing O_2 atmosphere for two hours. At this temperature and time, soda lime silicate glass produced a waveguide 85μm thick, which was highly multimode, and had a refractive index about 0.001. We tested the quartz for waveguiding using the prism coupling technique. No guiding was observed.

In the second experiment, electric field diffusion was attempted. The sample was heated for 12 hours in an oven at 700°C with an electric field of 200 V/cm applied across the electrodes. This is six times longer than normal, at twice the temperature and at twice the voltage needed in soda-lime-silicate glasses. During this time the "ion" current was monitored using a strip chart recorder (as normal procedure for electric field-assisted diffusion of glass waveguides). In contrast to the soda-lime-silicates, no ion current was observed. When tested by prism coupling, no waveguiding was seen. No further experimentation was attempted on quartz at this time. It should be pointed out that both "lithium stuffing" and proton bombardment remain possibilities for fabricating waveguides in quartz.


DAT:
ILME